REPORT DOCUMENTATION PAGE

Form Approved
OMB No. 0704-0188

1. REPORT DATE *(DD-MM-YYYY)*	2. REPORT TYPE	3. DATES COVERED *(From - To)*
18/Oct/2001	THESIS	

4. TITLE AND SUBTITLE
ADOPITIVE POLARIZATION OF ANTENNAS

5a. CONTRACT NUMBER

5b. GRANT NUMBER

5c. PROGRAM ELEMENT NUMBER

6. AUTHOR(S)
2D LT GRIFFIN BRIAN D

5d. PROJECT NUMBER

5e. TASK NUMBER

5f. WORK UNIT NUMBER

7. PERFORMING ORGANIZATION NAME(S) AND ADDRESS(ES)
UTAH STATE UNIVERSITY

8. PERFORMING ORGANIZATION REPORT NUMBER
CI01-270

9. SPONSORING/MONITORING AGENCY NAME(S) AND ADDRESS(ES)
THE DEPARTMENT OF THE AIR FORCE
AFIT/CIA, BLDG 125
2950 P STREET
WPAFB OH 45433

10. SPONSOR/MONITOR'S ACRONYM(S)

11. SPONSOR/MONITOR'S REPORT NUMBER(S)

12. DISTRIBUTION/AVAILABILITY STATEMENT
Unlimited distribution
In Accordance With AFI 35-205/AFIT Sup 1

13. SUPPLEMENTARY NOTES

14. ABSTRACT

20011115 138

15. SUBJECT TERMS

16. SECURITY CLASSIFICATION OF:			17. LIMITATION OF ABSTRACT	18. NUMBER OF PAGES	19a. NAME OF RESPONSIBLE PERSON
a. REPORT	b. ABSTRACT	c. THIS PAGE		71	19b. TELEPHONE NUMBER *(Include area code)*

Standard Form 298 (Rev. 8/98)
Prescribed by ANSI Std. Z39.18

ADAPTIVE POLARIZATION OF ANTENNAS

by

Brian D. Griffin

A thesis submitted in partial fulfillment
of the requirements for the degree

of

MASTER OF SCIENCE
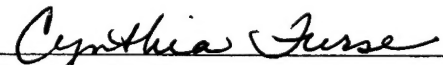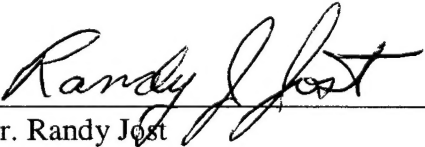
in

Electrical Engineering

Approved:

_____
Dr. Randy Haupt
Major Professor

_____
Dr. Cynthia Furse
Committee Member

_____
Dr. Randy Jost
Committee Member

_____
Dr. Thomas Kent
Dean of Graduate Studies

UTAH STATE UNIVERSITY
Logan, Utah

2001

Abstract

Adaptive Polarization of Antennas

by

Brian D. Griffin, Master of Science

Utah State University, 2001

Major Professor: Dr. Randy Haupt
Department: Electrical and Computer Engineering

Antennas whose polarizations are not aligned for optimal power transfer create a polarization mismatch and a loss in transferred power. A compensation for polarization mismatch is considered using a pair of crossed dipoles. One of the dipoles amplitude and phase is adjusted by a MATLAB optimization, and the Numerical Electromagnetic Code generates the electromagnetic response. Optimizing only for circular polarization produces losses in radiated power that offset the polarization correction. With minimum dipole separation, minor improvements are possible for $\theta < 15°$, but at larger angles the optimizer decreases the power transferred. The polarization optimization improves power transferred when the dipole spacing is increased. At 0.5 wavelength spacing, the increase in total gain is up to 17 dB. The optimization was modified to consider power transferred, and the power always increased up to a maximum of 2.0 dB at $\theta = 80°$. Crossed dipoles as the transmitter and receiver were also considered and they improved the power transferred.

(71 pages)

Acknowledgments

I would like to thank Dr. Randy Haupt for his support in the completion of this thesis and the masters program. He has always been available to answer questions or address concerns that I might have. I am grateful for his guidance and instruction over the past year, and the chance I have had to develop a relationship with him.

I would also like to thank my committee for their assistance and flexibility in helping me completing this thesis in the time constraints that have been imposed.

My parents and siblings also are deserving of my thanks as they have helped shape and make me the person I am today. My sincere thanks goes to my wife Rebecca for her willingness to put up with long hours and nights of homework. She has been a great support and motivation. She and Melissa are the joy of my life.

Brian Dan Griffin

Contents

List of Tables

List of Figures

Chapter 1

Introduction

The widespread use of satellites has increased the importance of the polarization of antennas. Satellite antennas use circular polarization to mitigate atmospheric losses of electromagnetic waves due to the Faraday rotation. This project focuses on the use of an optimization method to correct the polarization of an antenna system to transmit or receive circular polarization in any direction. This correction will compensate for any error caused by the antennas not having an accurate mechanical pointing system or being designed without a pointing system. These errors are caused by antenna misalignment, meaning the direction of propagation does not correspond to the antenna's designed direction for maximum gain and circular polarization.

To generate the desired circular polarization in this project, a pair of crossed dipoles is placed with one parallel to the x-axis and one parallel to the y-axis. The receiver will be an isotropic point source having circular polarization of the desired sense. The spacing between the dipoles and the presence of a ground plane will be considered in various configurations to understand the ability of the optimization to correct the polarization of the electromagnetic wave in a particular direction.

The optimization technique analyzes the response of a system to particular inputs based on a starting point and determines the effectiveness of the solution. It then chooses the best response and iteratively analyzes a new set of variations around that best solution. This new set of solutions is given an effectiveness, and the process repeats until the desired tolerances are met for the solution. The effectiveness may be determined using several factors, but for this project the cost will be based on first the desired sense,

next the axial ratio, and finally the gain in the direction of interest. The results of the
optimization for the various configurations of the dipoles will be analyzed to determine
any improvements in the system's performance and future work in the optimization of
circular polarized antennas.

1.1 Background

The polarization of an electromagnetic wave is the curve traced over time by the
electric field vector when observed in the direction of propagation. Balanis gives a
formal definition as, "that property of an electromagnetic wave describing the time
varying direction and relative magnitude of the electric-field vector at a fixed location in
space, and the sense in which it is traced, as observed along the direction of propagation"
[1]. Electromagnetic waves are in general elliptically polarized, with the electric field
vector tracing an ellipse. Two special cases of elliptical polarization exist as linear and
circular polarizations. Linear polarization occurs when the electric field vector follows a
line as a function of time, and circular polarization occurs when the electric field vector
traces a circle. Three factors used to classify polarization are axial ratio, tilt, and sense.
Axial ratio (AR) is defined as the ratio of the major axis to the minor axis of the ellipse
see Fig. 1.1. The tilt is the angle between the major axis and the x-axis, shown in Fig 1.1
as β. Finally the direction of rotation of the electric field vector around the ellipse is
defined as the sense, and it may be left or right handed. The Institute of Electrical and
Electronics Engineers (IEEE) definition of sense looks at the wave as it is receding and
its rotation is specified as either clockwise (right-handed) or counterclockwise (left-
handed).
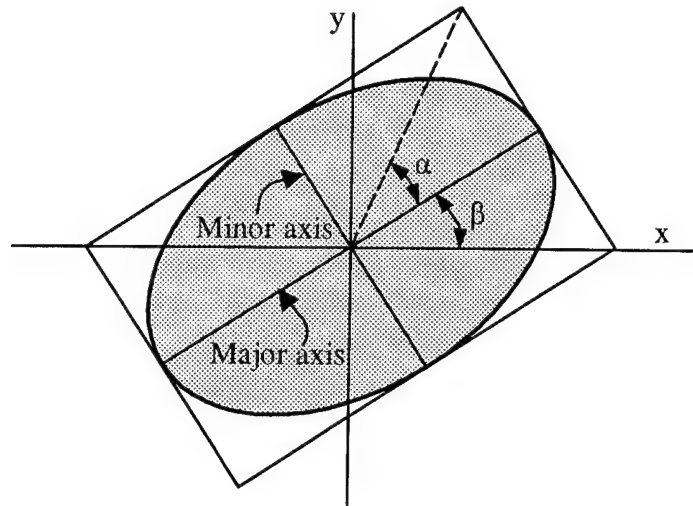
Fig. 1.1: Representation of elliptical polarization.

The Poincaré sphere is used to represent the polarization of a wave by characterizing a wave with longitude and latitude angles on the sphere as shown in Fig. 1.2. The point H on the sphere is the positive x-axis intercept for a rectangular coordinate system centered in the sphere. The equator of the sphere represents linear polarization with the tilt angle corresponding to the longitude. The positive z-axis pole represents a left-hand circular polarization, and the negative z-axis pole represents a right-hand circular polarization. The latitude on the sphere represents the axial ratio and the following equations describe the relationship between the parameters on the Poincaré sphere [2].

$$\cos 2\gamma = \cos 2\alpha \, \cos 2\beta \qquad (1.1)$$

$$\tan \delta = \tan 2\alpha \, / \, \sin 2\beta \qquad (1.2)$$

$$\tan 2\beta = \tan 2\gamma \, \cos \delta \qquad (1.3)$$

$$\sin 2\beta = \sin 2\gamma \, \sin \delta \qquad (1.4)$$
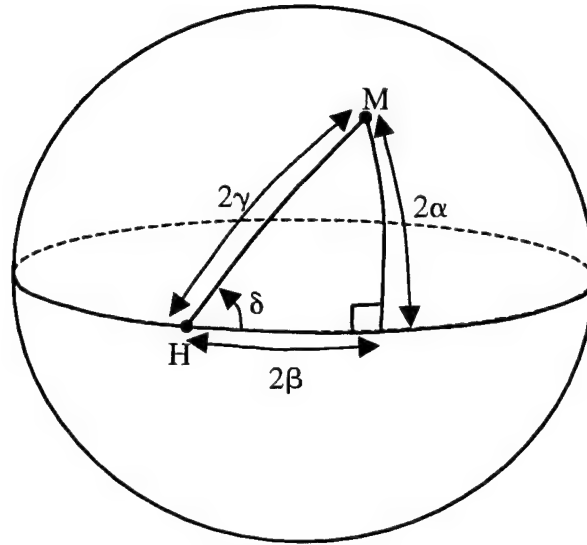
Fig. 1.2: Poincaré sphere representation of polarization.

Using these parameters it is possible to uniquely identify any polarization and determine its location on the sphere. Let M_a represent the polarization of an antenna (on the Poincaré sphere) and M_b the polarization of an incident plane wave. The angle between the two points on the sphere is the match angle, M_aM_b. Using this angle, a polarization loss factor F (for power) is determined using the following equation.

$$F = \cos^2 (M_aM_b / 2) \tag{1.5}$$

This loss due to the polarization mismatch between an antenna and the received wave forms the basic premise of this project.

1.2 Previous Work

The first investigations into the polarization of electromagnetic waves were in the field of optics, but the past 70 years has yielded significant research into polarized electromagnetic waves at radio frequencies. The earliest research into the polarization of radio waves focused on the earth's magnetic field and ionosphere. The deliberate

polarization of electromagnetic waves at radio frequencies started during World War II. As part of these investigations, Harrison and King considered the polarization of electromagnetic waves, when they analyzed the reception of a linear antenna in an electric field. One part of their analysis deals with using a pair of crossed dipoles to produce an elliptically polarized field and the fact that, "[an] elliptically polarized electric field can always be decomposed into two components which are fixed in space and which differ in phase, magnitude, and direction" [3]. This ability to characterize an elliptically polarized wave using two components allows a pair of dipole to generate a wave of any polarization, although the wave may be limited by the dipoles' orientation. Harrison and King also point out a key problem associated with receiving an elliptically polarized wave when the antennas are not perpendicular to the direction of propagation. They state, "it is clear that it is imperative to know the complex expression and not just the magnitude of the effective height of a particular receiving antenna whenever this does not lie in an equiphase plane of an elliptically polarized electric field" [3]. This recognizes the resulting phase challenges for a linear antenna that is receiving a plane wave, when the antenna is not perpendicular to the direction of propagation.

Sichak and Milazzo provided the next major contribution to the understanding of circular polarization in 1948. They provided a method to find the voltage, "induced on an elliptically polarized receiving antenna located in the field of an elliptically polarized wave" [4]. Using their method, the transmitting and receiving antennas must have the same polarization, as determined when each is acting as a radiator, to achieve the best reception. Their method also points out that the energy transferred between two elliptically polarized antennas will depend on both the polarization and the antenna

pattern. They also used crossed dipoles as a method to develop circular polarization producing, "both right-handed and left-handed circular polarization simultaneously in different directions" [4]. These two polarizations are in the two directions perpendicular to the plane containing the crossed dipoles.

Yung-Ching Yeh published a method of antenna design in 1949 that also considered the polarization of antennas [5]. He started from the assumption that the incoming wave is known, and considered the effect of the earth's fields on the propagation of the wave. For waves that arrive with an elliptical polarization the suggestion is made that two linearly polarized antennas should be designed with maximum gain in the desired direction, and then their relative phases should be adjusted to achieve the maximum power received. This method works well for waves that may be measured and when the antennas are properly aligned with the direction of propagation.

A contribution by George Sinclair in 1950 added significantly to the understanding of electromagnetic waves and the characterization of their polarization [6]. He demonstrated that an elliptically polarized electric field my be resolved into, "its three spherical components at each point in space." This allows the propagation and polarization to be characterized by a specific coordinate system using three vectors. Morgan and Evans also considered the use of three vectors in 1951 [7]. Their analysis gave the equations that produce any electromagnetic wave of any polarization in any direction based on the three orthogonal components. They also considered the two-component case, but only in the direction of propagation. Compton conducted a more recent look at the three-component characterization using a least-mean-square (LMS) adaptive algorithm [8]. His design used three orthogonal dipoles to receive a desired

signal from a specific direction and with specific polarization and to reject an interfering signal from a different direction and/or polarization.

The Institute of Radio Engineers (I.R.E.) published a major compilation of works on elliptical polarization in 1951. Rumsey produced the first article in the compilation about elliptically polarized antennas and transmission between them. Two items he discussed are relevant to the current work. The first is a statement about how the, "orientation and axial ratio of the *effective* ellipse," changes by rotating an elliptically polarized antenna [9]. This statement applies in general to any rotation of an elliptically polarized antenna, but the only case he considers is a rotation about the direction of propagation. The second item relevant to the current work is the use of polarization parameters as a way to determine the maximum power transfer between antennas.

The next paper in the 1951 work by the I.R.E. was written by Deschamps on a way to characterize the polarization of a wave using a geometric representation. The method proposed was that of a Poincaré sphere, and this method of characterization has continued to be widely used. This representation was originally developed for problems in optics, but applies directly to the polarization of electromagnetic waves. The representation uses an ellipticity angle, α, and an orientation angle, β as previously discussed (see Fig. 1.1 and 1.2). "Poincaré's representation consists in handling 2β and 2α as longitude and latitude of a point on a sphere" [10]. This representation allows the relative distances between two polarizations to be compared and conclusions developed. One unique point given by Deschamps is the ability to determine where the current polarizations of two antennas fall on the Poincaré sphere and then to, "modify their relative phasing or their relative amplitude to approach a certain goal" [10]. This is an early look at adapting the

antennas to fix imperfections, but only considers antennas that have no pointing error or are aligned with the direction of propagation.

Kales contributed the third paper for the 1951 compilation and made an important observation about the use of orthogonal linearly polarized fields to produce an elliptically polarized field. He stated that an arbitrary axial ratio and sense of rotation can be produced with the two linearly fields by having either, "(a) the two components … in phase quadrature and the amplitudes … properly chosen, or (b) the two components … equal in amplitude and the phase … properly chosen" [11]. This is directly applicable to the use of crossed dipoles and setting up a specific elliptically polarized wave, but only the case of proper antenna alignment is considered. Kales also developed a term called the polarization efficiency to determine the power transferred between two polarized antennas. In general, this compilation by the I.R.E. was one of the foundation documents for the understanding and characterization of polarization and its application to antennas.

The next few articles deserve brief attention as they added to the understanding and practical uses of polarization, but they have minor application to the current work. The first was another look at a geometric representation of polarized and partially polarized waves by Bolinder in 1967 [12]. Next, Dudzinsky addressed the use of polarization discrimination, the use of two signals with different polarizations, for satellite communications in 1969 [13]. Finally, Chu examined the use of polarization orthogonality in radio communications and a method to adjust the amplitude and phase of a system to remove an undesired nonorthogonality caused by imperfect antenna elements [14].

A paper published in 1974 by Marshall has direct application to the current work [15]. The focus of his paper was a method to correct for the polarization change caused by rain in a communication channel. The system was using circular polarization with a pair of crossed dipoles as the transmitting source. By adjusting the magnitude and phase of the dipoles it is possible to create a circular polarized wave after the signal has passed through the polarization modification caused by the rain. This differs from the current work in the source of polarization error, but the method of correcting the polarization through the adjustment of amplitude and phase is the same. His conclusion reveals the ability of a communication link to correct for a polarization distortion, as is the focus of this work.

Nathanson also considered the effect of rain polarization on signals and developed a method to adapt a radar system to overcome the effects of the rain [16]. He examines the use of two antennas with opposite polarization sense and a method of signal processing to cancel the polarization effect caused by the rain.

Kummer and Gillespie produced a major contribution to the understanding of an antenna's polarization as part of a measurements guide in 1978 [17]. They reiterated that the polarization of a plane wave must occupy a point on the Poincaré sphere. They show that the antennas used to measure the wave do not have precisely known polarizations, and thus introduce an error into measurements. To address this issue they discussed a three-antenna method that was developed to find the absolute polarization of an antenna, where the three antennas are calibrated with each other to determine a complex-polarization ratio. These ratios completely describe the response of the three-antenna set, and then the antenna set may be used to precisely determine the unknown signal. Other

methods are presented that do not yield an absolute polarization, but may be used if some information is previously known about the signal. In general, their focus was on the practical measurement of antennas, and understanding the steps that are needed to completely characterize an antenna.

In 1981 Compton published a work using crossed dipoles in an array that has application in receiving signals when there is an antenna misalignment [18]. His system consists of two pairs of crossed dipoles separated by some distance, but with their dipole elements all in the same plane. With this setup an LMS algorithm was used to optimize the array for a desired signal, and reject an interfering signal. Most of the work was done with the desired signal arriving perpendicular to the plane containing the pairs of crossed dipoles, but he does consider the case of the desired signal coming from another direction. This misalignment of the desired signal is the focus of the current work and Compton's treatment of this case shows that signal discrimination is possible. His method does require the two sets of crossed dipoles, because the LMS algorithm needs the phase information provided by their physical separation to deal with misaligned signals. Compton's work is closest to the present work in his consideration of crossed dipoles and the ability to handle a directional misalignment of the desired signal.

Pozar and Targonski, and then Parekh each published a paper discussing crossed dipole polarization systems [19,20]. They considered errors that are introduced when using two orthogonal components to generate any elliptical polarized wave. These errors include: the amplitude and/or phase errors in driving the antenna elements, the unwanted cross-polarization of the antenna elements, the error in achieving orthogonality between the two antenna elements, and the polarization error resulting from the signals not being

perfectly linear. Each of these errors must be considered in the development of an elliptically polarized system using orthogonal components.

Pozar also published a paper in 1992 that dealt with circular polarization produced by an infinite array [21]. He considered several types of elements that could be used to construct an array with circular polarization. He also produced results that indicate the limitations of these arrays in maintaining a desired axial ratio at different scan angles. He showed that some array elements, particularly rectangular patches, do not maintain a circular polarized wave at scan angles greater than 20°. A sampling of other works looking at generating circular polarization using various antenna setups and feed systems is found in [22-24].

A recent article dealing with circular polarization in different directions was give by Tanaka in 1999 at the IEEE Antennas and Propagation Society International Symposium [25]. He presented a phased array that adjusts the desired polarization based on the tilt of the antenna elements within the array. This method uses an array of antennas each linearly polarized and each with a different angle of rotation about the axis perpendicular to the antenna's linear polarization. With the difference between the spacing of the elements and the different angles a set of equations that may be solved to produce the desired polarization in a desired direction.

Chapter 2

Crossed Dipole Simulation Setup

To simulate the crossed dipole setup and allow various optimization routines, a MATLAB script was written to control the parameters and display the resulting data. This script has several sections including: the setup of the geometry of the problem, the numerical optimization, and the display of the resulting data. This project's optimization will be foremost based on the desired sense, then the axial ratio, and finally the gain in the direction of interest. This process is summarized in the block diagram shown in Fig. 2.1 and the complete code is in Appendix A.
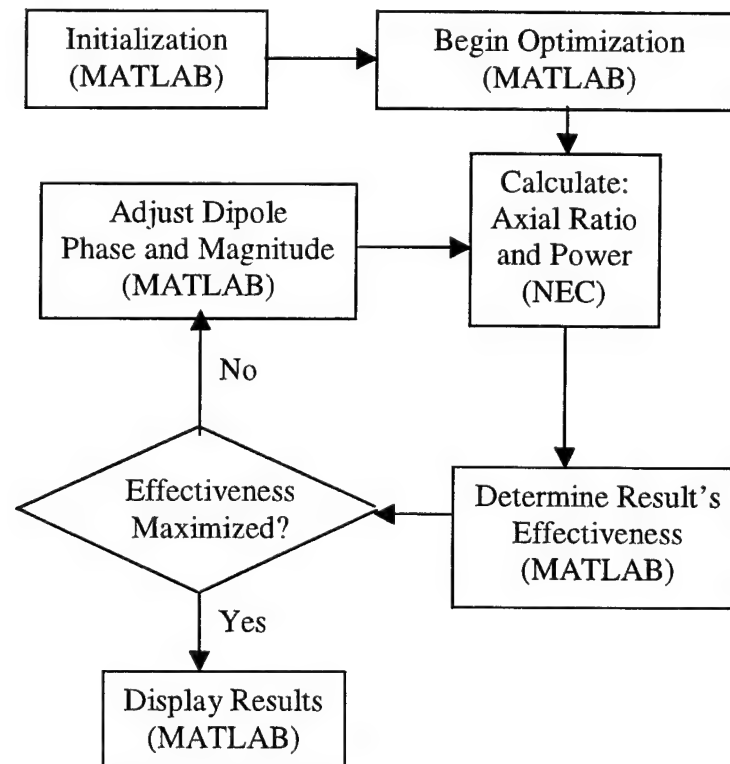
Fig. 2.1: Block diagram of the MATLAB and NEC optimization.

The first challenge involves setting up the geometry of the problem or the initialization. To do this there are several parameters that are specified by the user. Some of these don't change very often, and include the frequency of operation, the input filename, and the wire radius. On the other hand, the optimization point is where the isotropic receive antenna is located with the desired sense of circular polarization, and it is specified every time the script is run, see Fig. 2.2. To specify the optimization point the user enters theta and phi. The user also sets the desired sense for the circular polarization (Right hand or Left hand). Based on the theta angle and the desired sense, the MATLAB code determines what the starting values should be for the real and imaginary parts that drive the second dipole. Other calculations that are based on the user-defined parameters include: the physical separation of the dipoles along the z-axis and the dimensions of the dipoles. The separation takes on several values as different
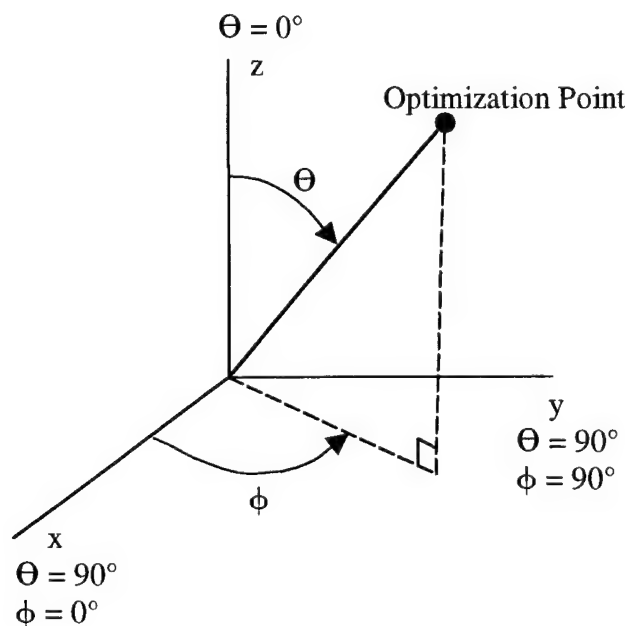
Fig. 2.2: Spherical coordinate system and optimization point.

configurations were considered. For those results specified as minimum separation, it is equal to doubling the wire radius and adding an additional quarter wire radius. This simulates a setup that is similar to the real world where the dipoles are usually not in exactly the same plane. The dimensions of the dipoles are calculated by finding the wavelength of operation in free space. With this result the length of each dipole is set to be half of the wavelength. All of these parameter calculations are completed prior to starting the optimization.

The next requirement was the creation of the NEC input file that contained the desired antenna dimensions, the frequency of operation, and the point at which the antenna's pattern is being optimized. This was done as part of a separate MATLAB script because it will be called several times during the optimization. This script puts the crossed dipoles in the xy plane, with one antenna along the x-axis and the second vertically separated, but oriented parallel to the y-axis see Fig. 2.3. The first dipole is fed with a voltage of one and no phase shift.
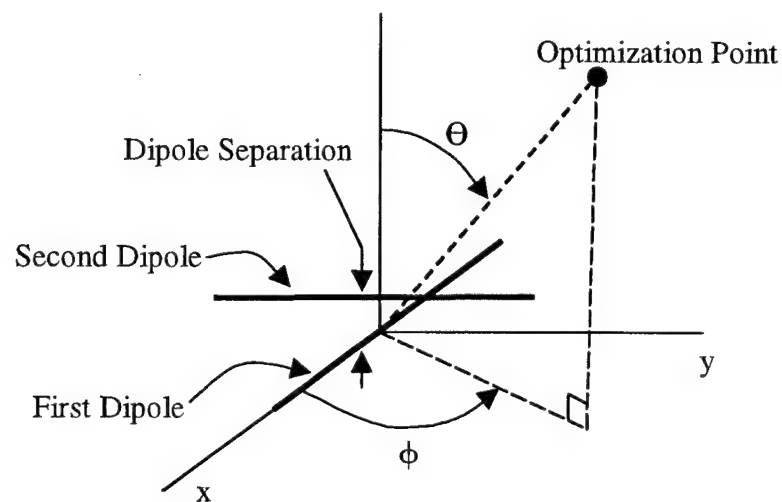
Fig. 2.3: Geometry of the crossed dipoles.

The next step was to determine the starting magnitude and phase on the second dipole. For all of the possible cases, the magnitude starts at one, but the phase changes between ±90° depending on which hemisphere the optimization point is in and the desired sense of the circular polarization. This sets the initial conditions of the system and the initial gain. The optimization may adjust the magnitude of the second dipole to values greater than one, but the important result is the ratio of the magnitudes between the two dipoles. Therefore, a power divider would likely be used in a real world setup. The NEC code is executed once to provide the starting axial ratio, tilt angle, and sense for later display. Next, the MATLAB script moves to the numerical optimization.

There are several possible techniques that may be used to optimize this circular polarization problem. To maintain the simplicity of this script, a built in MATLAB function called 'fminsearch' was used to perform the optimization. The optimization problem requires the magnitude and the phase of the second dipole to be adjusted to achieve circular polarization at the chosen optimization point. 'Fminsearch' is the only MATLAB function that will optimize with multiple input values, and is therefore appropriate for adjusting both the magnitude and the phase. For this function there are two separate MATLAB scripts that work within the optimization: an optimization function called 'AR_optimize' and the script that creates the input file for NEC.

The optimization function takes the current magnitude and phase for the second dipole and calls the second script to create a new NEC input file for the given set of parameters. With this input file, the NEC program itself is called and it produces several output files containing the simulated results of the crossed dipoles [26]. MATLAB then extracts the axial ratio, the tilt, and the sense from a special file created by modifying the

NEC source code. It also extracts the relative power of the signal at the optimization point using another NEC file.

The modification of the NEC source code was part of a previous project by You Chung Chung. With his assistance I underwent a quick tutorial in programming in FORTRAN and then modified the source code to produce the parameters relating to circular polarization [27]. These parameters include axial ratio, tilt, and sense. This data was written to a separate file named 'Polar' to interface with MATLAB. This modification allowed MATLAB to easily import the data and run the optimization routine. A similar setup was used to extract the power information. The disadvantage to this setup is the multiple disk operations required during the optimization process, which slows down the optimization. To increase performance, the NEC source code was further modified to reduce the number of data files produced.

With these results from NEC, the optimizer then looks at the axial ratio at the optimization point and adjusts the magnitude and phase of the second dipole to force circular polarization at that point. The user, in the setup of 'fminsearch' within MATLAB, may set the tolerance required for the final axial ratio or the number of iterations to try. At the end of this optimization the magnitude and phase that produced the desired result is returned.

After the optimization is completed MATLAB is used to produce plots of the resulting data. The first figure is a three dimensional picture of the optimization point in relation to the crossed dipoles. This plot displays the starting axial ratio and tilt at the optimization point and the final axial ratio and sense (Fig. 2.4). The plot also displays the magnitude and phase driving the second dipole that produced the circular polarization.
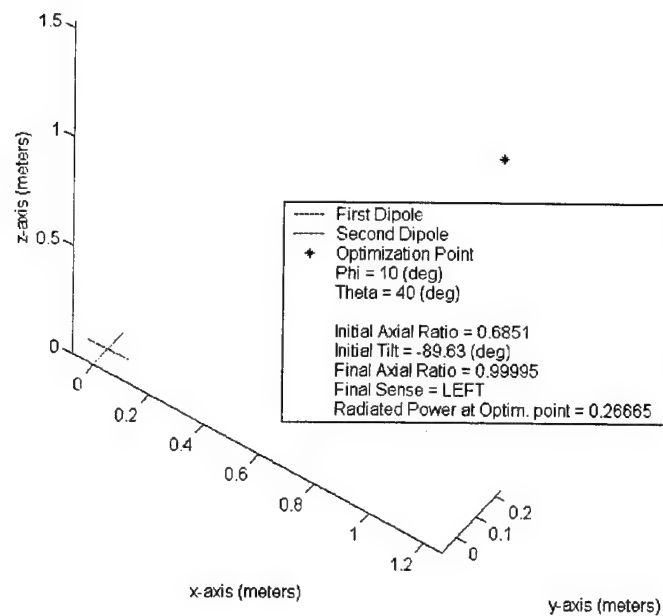
Fig. 2.4: Three dimensional, optimization data display.

This allows the user to visualize the results of the polarization optimization. The second figure is of the axial ratio at each step of the optimization, and allows the user to see how the axial ratio changes (Fig. 2.5).

The final step of the MATLAB script is to produce a NEC output file with the complete antenna pattern for the crossed dipoles for further analysis. Final cleanup includes the removal of all unnecessary files created during the optimization.

After significant data was taken using the initial MATLAB script, the optimization was further modified in the determination of effectiveness for a particular solution. The modification takes into account the loss of radiated power due to the optimization of polarization. This new effectiveness equation maximize the benefits to be found in correcting the polarization and minimize the loss due to the adjustment of the antenna
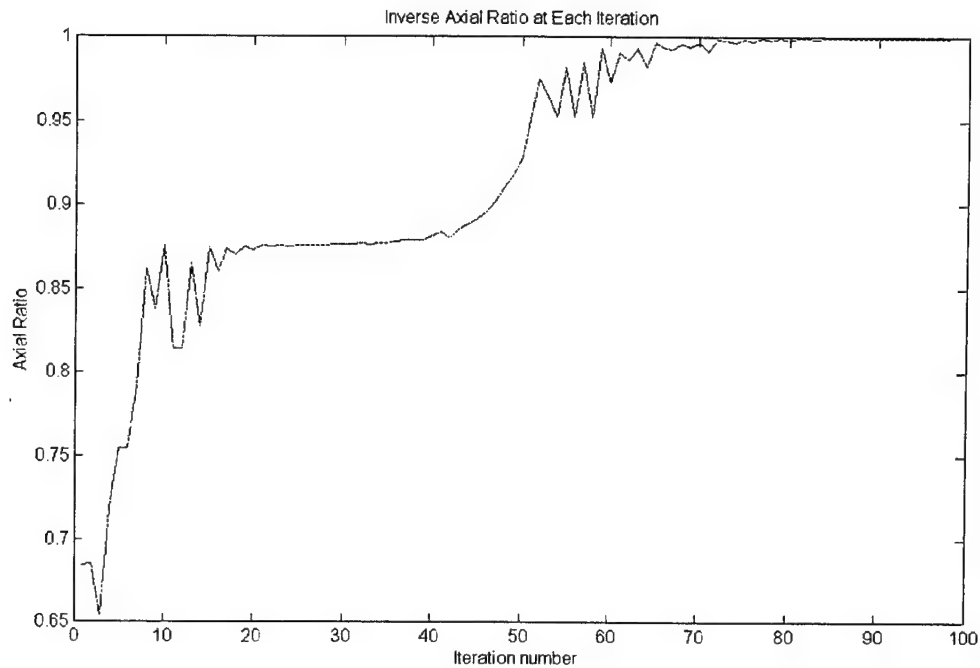
Fig. 2.5: Inverse axial ratio at each iteration of the optimization.

pattern. In other words, the effectiveness is based on the power transferred, not just the polarization. The improved equation then determined if a polarization adjustment is appropriate for a given configuration to maximize the total gain. Using this revised optimization, additional data was taken for comparison to the previous results.

Further modifications to the effectiveness equation may be accomplished in the 'AR_optimize.m' script using the 'test' variable. These modifications may include the addition of environmental factors present in the communication link. This would provide a way for the optimization to account for such things as the Faraday rotation. This modification was not completed for this thesis, but may be of interest in the future.

Chapter 3

Simulation Results

Several configurations of crossed dipoles were considered in an attempt to characterize and understand the limits of an adaptive system. Each of these results will be examined and conclusions presented, see Appendix B for complete tables of data.

3.1 Ideal Crossed Dipoles

First let us consider a pair of crossed dipoles in an ideal configuration, where they are both in the xy-plane see Fig. 2.3. With this setup, consider the resulting polarization at various angles and the possibility of adjusting the amplitude and phase of one of the dipoles to create circular polarization in any direction. The antenna pattern for the dipole pair when configured to create circular polarization at $\theta = 0°$ is shown in Fig. 3.1, with the figure angles indicating the point of view for the pattern. Note these patterns are only for the top half of the radiation pattern, with the lines representing the dipoles' location.

View $\phi = 104°$
View $\theta = 48°$

View $\phi = 62°$
View $\theta = 24°$
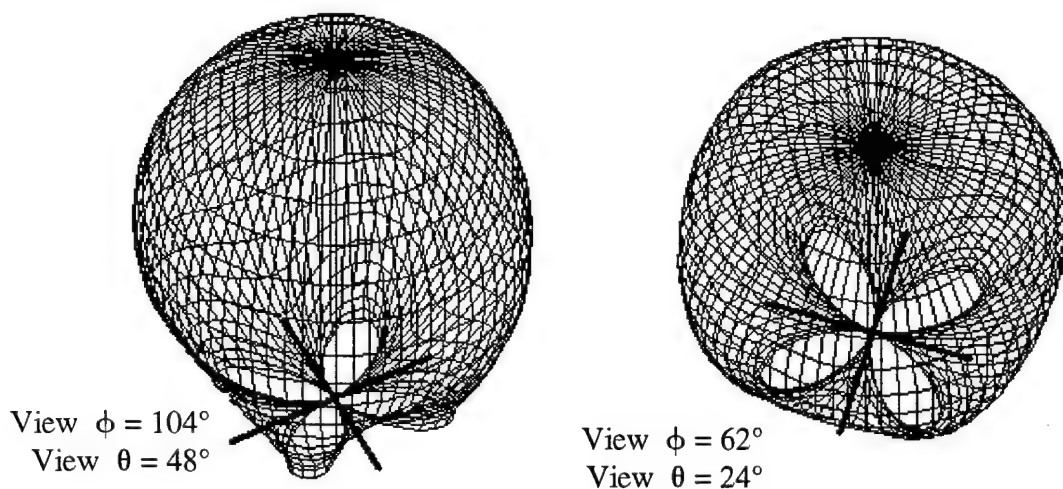
Fig. 3.1: Ideal crossed dipoles antenna pattern.

These results are as expected for a pair of dipoles, with the deep nulls at the ends of the dipoles. NEC generates the inverse axial ratio of any point in the antenna pattern, and for this pair of dipoles the inverse axial ratio follows a cosine curve as θ varies from $0°$ to $90°$. This result is shown in Fig. 3.2 as a plot of the inverse axial ratio vs. θ. Using this information it is possible to determine the increase in gain that is possible by correcting the polarization of the antennas to match a circular polarized wave coming from any direction. This gain is shown in Fig. 3.3 for the different values of theta. In the simulated results the adaptation of the amplitude and phase of the y-axis dipole yields a circularly polarized wave in any direction up to a value of $\theta = 85°$. This seems to indicate that this method of increasing the gain of a pair of crossed dipoles will be successful. This successful increase of the gain will be examined in greater detail in the consideration of a more realistic setup of the crossed dipoles.
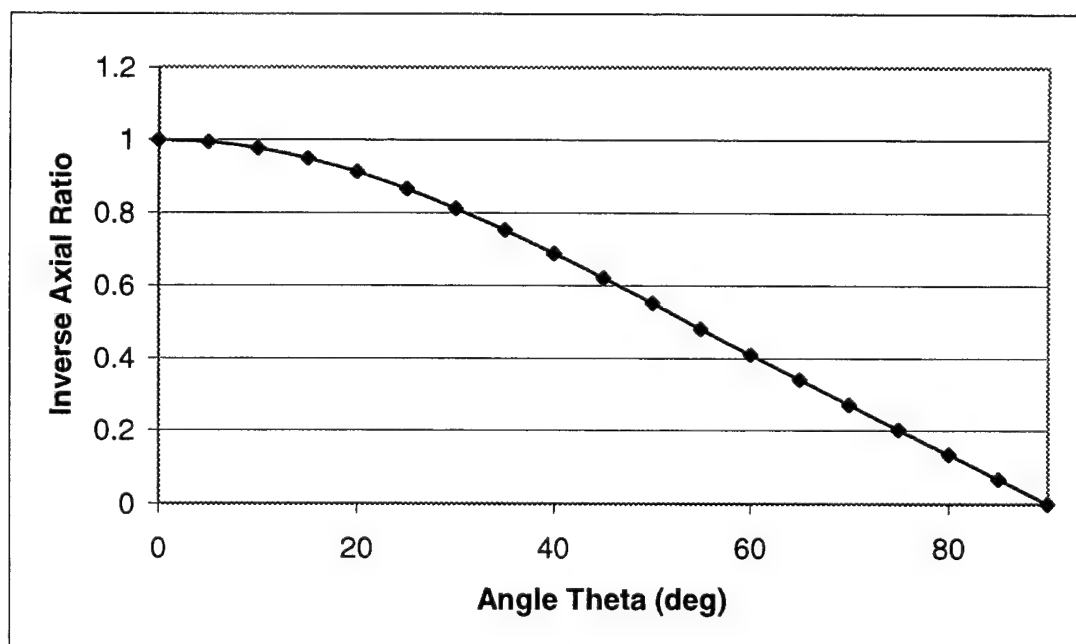
Fig. 3.2: Inverse axial ratio of ideal crossed dipoles.
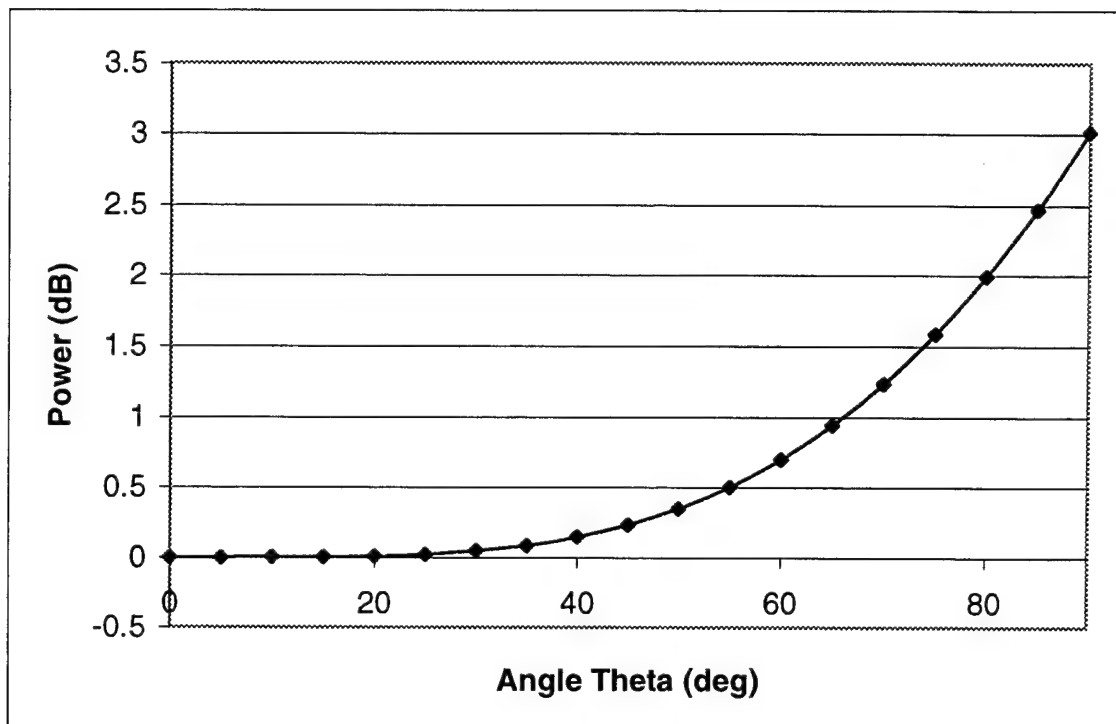
Fig. 3.3: Possible gain improvements for different angles of misalignment.

3.2   Non-Ideal Crossed Dipoles

Next let us consider a less ideal set of crossed dipoles, where the two are not co-located in the xy-plane, but they have some vertical separation due to the thickness of the antenna and the need to maintain a physical separation (see Fig, 2.3). This separation was determined by using the radius of the wire for the antenna elements, and was equal to two times the radius of the wire plus another fourth of a wire's radius. Therefore, the separation between the elements is minimal. Using this configuration the optimization determined that a magnitude of one and a phase of 88.6406° was required to produce circular polarization at $\theta = 0°$. The antenna pattern produced using this non-ideal set of crossed dipoles is shown in Fig. 3.4, note the change in the nulls of the pattern. Using this pattern as the baseline for optimization in other directions, it was once again

Fig. 3.4: Non-ideal crossed dipoles antenna pattern.

View ф = 29°
View θ = 75°

View ф = 55°
View θ = 159°
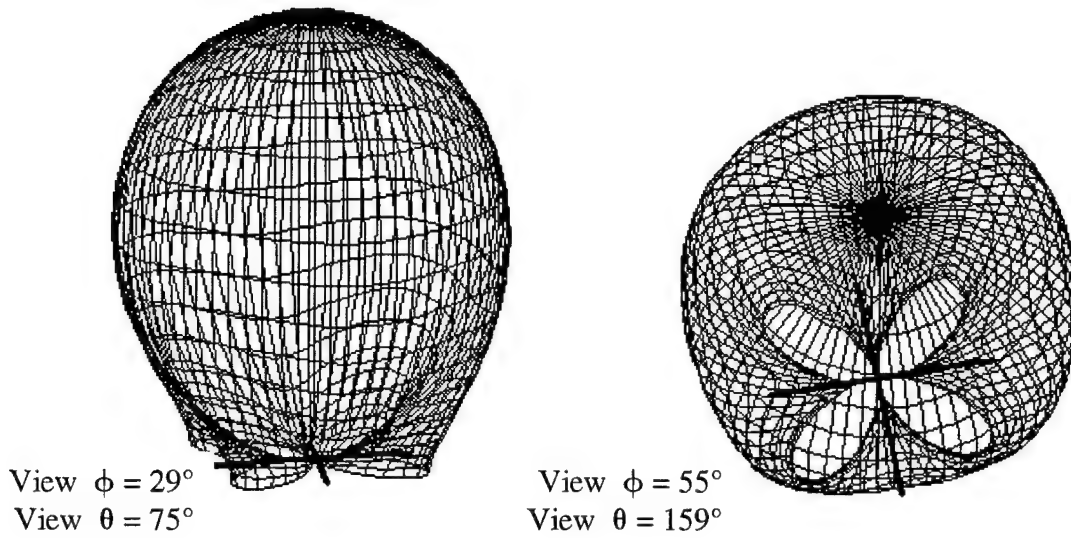
determined that circular polarization could be produced in any direction, and the resulting polarization gain follows closely that of the ideal crossed dipole case. The breakdown of this optimization setup occurs when the change in the antenna pattern is taken into account after the optimization has adjusted the magnitude and phase driving the second dipole. To produce the circular polarization at any point the location of the nulls in the antenna pattern change as the difference in the phase between the two dipoles changes.

Consider the case where the circular polarization is desired in the direction $\theta = 35°$ and $\phi = 0°$. The optimizer determines that a magnitude of 0.75257 and a phase of 89.0827° are required to achieve circular polarization. Using these values, a gain of 0.09 dBi is achieved by correcting the polarization, but a radiated loss of -0.34 dBi occurs due to the change in the antenna pattern. Therefore the net gain due to optimization is –0.24 dB. The change in the antenna pattern is shown in Fig. 3.5, note the new placement of the nulls. This failure to increase the gain remains throughout the $\phi = 0°$ portion of the

View φ = 0°
View θ = 35°

View φ = 204°
View θ = 145°
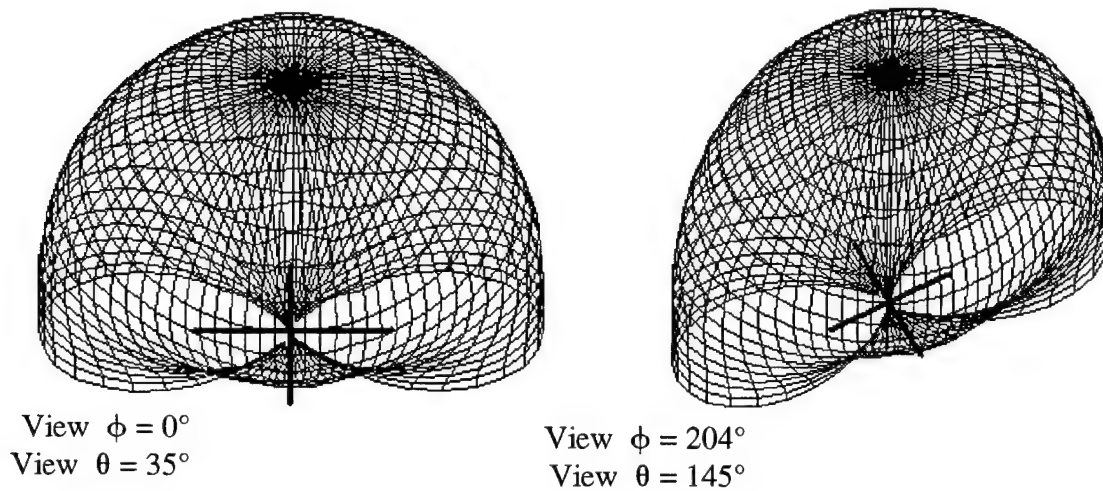
Fig. 3.5: Antenna pattern after optimization at θ = 35° and φ = 0°.

pattern. There is some improvement in the results when the misalignment occurs in the φ = 45° plane. In this case, the losses in the antenna pattern power balance with the gains in the optimized polarization for θ < 15°. For larger values of θ the radiation loss is greater than the polarization gain for a given value of θ. The resulting antenna pattern for θ = 20° and φ = 45° is shown in Fig. 3.6 where the magnitude on the second dipole is

View φ = 0°
View θ = 35°

View φ = 45°
View θ = 50°
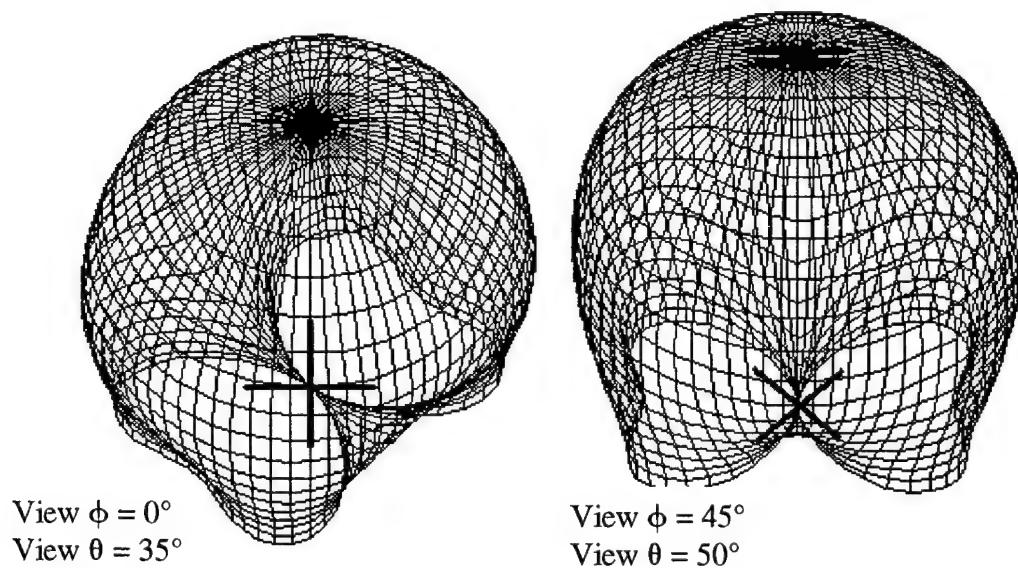
Fig. 3.6: Antenna pattern optimized for θ = 20° and φ = 45°.

0.99998 and the phase is 78.8196°. Note the null at $\phi = 45°$.

3.3 Non-Ideal Crossed Dipoles With a Ground Plane

To further examine the use of crossed dipoles, a ground plane was introduced into the problem with the non-ideal crossed dipoles. This configuration was used for spacing between the ground plane and the dipole pair of 0.25, 0.375, and 0.15 wavelengths. The addition of the ground plane creates a reflection of the crossed dipoles, and the optimizer was once again able to produce a circular polarized wave in all directions where $\theta > 85°$. Each of these configurations yielded a larger gain in the direction perpendicular to the dipoles as expected for a reflected wave. All of these configurations suffer from the same gain problems as the single crossed dipoles, in that the optimization increases the gain due to the polarization, but decreases the radiated power in the desired direction resulting in a loss of total power.

3.4 Crossed Dipoles with Larger Separations

The one area where the adaptation of the antennas produces increases in gain relative to the starting pattern occurs when the spacing between the dipoles increases beyond 0.1 wavelength. This case may occur when the physical requirements of a system are such that the dipoles must have a larger separation, but still may be oriented as a crossed pair.

To explore this configuration, the dipole pair was first setup with a separation of 0.2 wavelengths and then optimized to produce a circular polarized wave in the $\theta = 0°$ direction. The results of this setup are shown in Table 3.1 for those angles that yield a total gain as a result of the optimization. These results indicate that small gains are achieved when the optimization routine adjusts the crossed dipoles to correct for the

Table 3.1: Optimized Results for Dipole Spacing of 0.2 Wavelengths

θ	φ	Pre-Optimization Pattern Gain (dBi)	Inverse Axial Ratio	Tilt Angle (deg)	Sense	Pattern Gain after Optimization	Power Loss by Polarization Mismatch (dBi)	Total Transferred Power Gain or Loss (dB)
0	45	2.18	1.00	45.63	LEFT	2.18	-1.7E-09	1.7E-09
5	45	2.16	0.999	1.1	LEFT	2.15	-1.0E-06	-0.01
10	45	2.08	0.996	0.28	LEFT	2.08	-1.6E-05	1.6E-05
15	45	1.95	0.992	0.13	LEFT	1.95	-7.3E-05	7.3E-05
20	45	1.77	0.986	0.08	LEFT	1.77	-0.0002	0.00020
25	45	1.52	0.981	0.05	LEFT	1.53	-0.00042	0.010
30	45	1.21	0.975	0.04	LEFT	1.23	-0.0007	0.021
35	45	0.83	0.971	0.04	LEFT	0.86	-0.00097	0.031
40	45	0.36	0.969	0.03	LEFT	0.40	-0.0011	0.041
45	45	-0.19	0.970	0.04	LEFT	-0.15	-0.001	0.041
50	45	-0.86	0.977	0.05	LEFT	-0.82	-0.00058	0.041
55	45	-1.66	0.992	0.15	LEFT	-1.64	-7.1E-05	0.020
60	45	-2.61	0.982	89.93	LEFT	-2.66	-0.00037	-0.050
0	0	2.18	1.00	-89.39	LEFT	2.18	-1.7E-09	1.7E-09
5	0	2.16	0.992	70.04	LEFT	2.16	-6.3E-05	6.3E-05
10	0	2.08	0.970	70.01	LEFT	2.08	-0.001	0.0010
15	0	1.96	0.934	70.05	LEFT	1.95	-0.0050	-0.0050
20	0	1.8	0.886	70.15	LEFT	1.76	-0.016	-0.024

circular polarization error. In this case the gains are not generally caused by the polarization mismatch, but because the optimization increased the radiated gain of the antenna pattern in the desired direction. It is interesting to observe the antenna pattern at the point with the greatest gain, θ = 40° and φ = 45°, as shown in Fig. 3.7.

Next consider the case where the spacing between the dipoles is 0.5 wavelength. This setup yields additional benefits as a result of the optimization in both radiated power in the desired direction and the power gained by correcting the polarization mismatch. The results at selected points in the antenna pattern are shown in Table 3.2. Note that much of the total gain increases in this setup occur as a result of the large errors in the polarization at some of the values of θ > 55°.

View φ = 48°
View θ = 125°
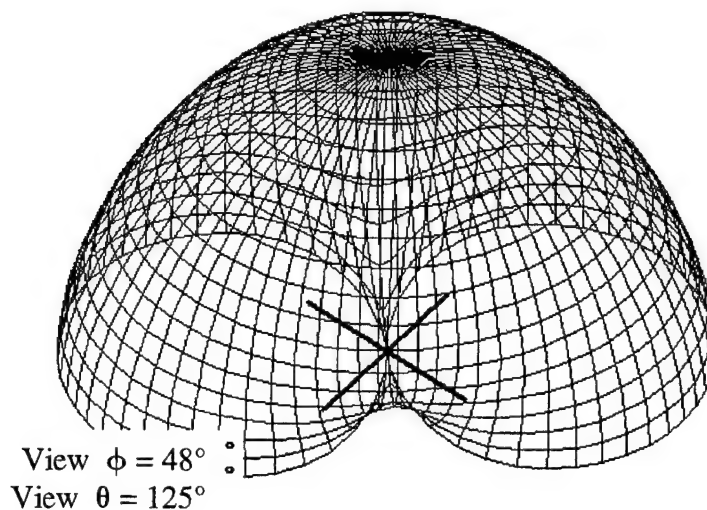
Fig. 3.7: Antenna pattern for θ = 40°, φ =45°, and spacing of 0.2 wavelengths.

Table 3.2: Optimized Results for Dipole Spacing of 0.5 Wavelengths

θ	φ	Pre-Optimization Pattern Gain (dBi)	Inverse Axial Ratio	Tilt Angle (deg)	Initial Sense	Pattern Gain after Optimization (dBi)	Power Loss by Polarization Mismatch (dBi)	Total Transferred Power Gain or Loss (dB)
0	0	2.18	1.00	-43.09	LEFT	2.18	-9.8E-10	9.8E-10
25	0	1.60	0.715	58.25	LEFT	1.51	-0.12	0.03
35	0	1.12	0.507	59.09	LEFT	0.76	-0.44	0.08
45	0	0.58	0.291	60.96	LEFT	-0.38	-1.14	0.18
50	0	0.32	0.186	62.54	LEFT	-1.15	-1.68	0.21
55	0	0.07	0.086	64.75	LEFT	-2.10	-2.33	0.16
60	0	-0.16	-0.004	67.78	RIGHT	-3.25	-3.05	-0.04
65	0	-0.36	-0.077	71.76	RIGHT	-4.69	-3.74	-0.59
75	0	-0.65	-0.137	81.66	RIGHT	-8.92	-4.38	-3.89
10	45	2.08	0.968	0	LEFT	2.08	-0.0011	0.0011
20	45	1.74	0.879	0	LEFT	1.77	-0.02	0.05
30	45	1.06	0.748	0	LEFT	1.23	-0.09	0.26
35	45	0.54	0.669	0	LEFT	0.86	-0.17	0.49
40	45	-0.13	0.579	0	LEFT	0.40	-0.30	0.83
45	45	-0.98	0.477	0	LEFT	-0.15	-0.51	1.34
50	45	-2.03	0.354	0	LEFT	-0.82	-0.89	2.10
55	45	-3.30	0.202	0	LEFT	-1.64	-1.59	3.25
60	45	-4.70	-0.001	0	RIGHT	-2.66	-3.02	5.06
65	45	-5.96	-0.291	0	RIGHT	-3.95	-6.34	8.35
70	45	-6.52	-0.743	0	RIGHT	-5.63	-16.7	17.6
75	45	-5.99	-0.649	-90	RIGHT	-7.91	-13.6	11.7
80	45	-4.72	-0.308	-90	RIGHT	-11.3	-6.60	0.06

View $\phi = 0°$
View $\theta = 45°$
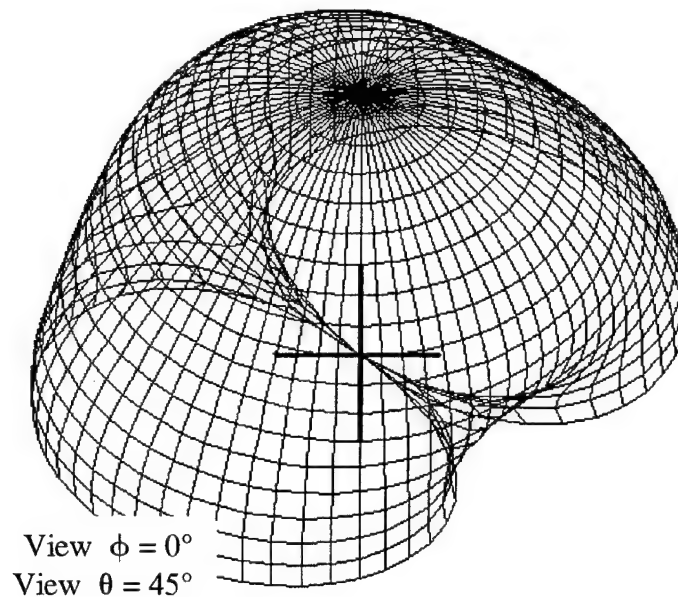
Fig. 3.8: Antenna pattern for $\theta = 70°$, $\phi = 45°$, and spacing of 0.5 wavelengths.

In this setup, the largest gain after the optimization occurs at $\theta = 70°$ and $\phi = 45°$, the radiation pattern at this point after the optimization is shown in Fig. 3.8. This pattern indicates that the null is still being moved to correspond to the direction of the optimization point, but due to the large mismatch in the polarization between the initial setup and the optimized setup, the gain resulting from the optimization is 17.6 dB.

Finally, other spacings between the dipoles were considered with varying results. For a spacing of 0.25 wavelengths, the results follow that of the ideal crossed dipole almost exactly, with no gain resulting from the optimization. For a spacing of 0.35 wavelength the gain is similar to that of the 0.2 wavelength spacing. An interesting case occurs when the spacing is larger than one wavelength. Using a spacing of 1.2 wavelengths the optimization produces a gain of 7.8 dB over the initial signal at $\theta = 50°$ and $\phi = 0°$. This setup produces a unique radiation pattern as shown in Fig. 3.9. Note the location of the nulls from both dipoles and how the second has moved to create the
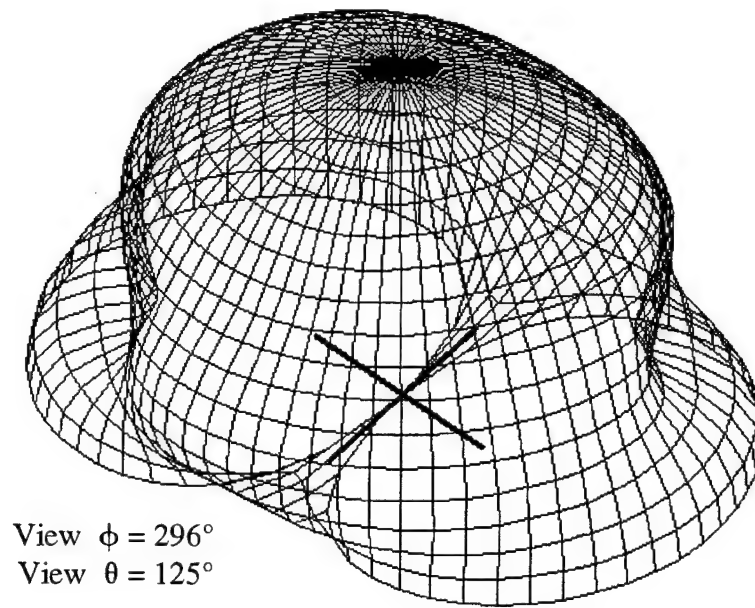
Fig. 3.9: Antenna pattern for θ = 50°, φ =0°, and spacing of 1.2 wavelengths.

circular polarization at the desired point. The improvements in the gain resulting from optimization result from the large mismatch in the polarizations at the point of interest. These large mismatches do not occur in the crossed dipole case with a spacing less than 0.1 wavelength. Therefore, the only advantage produced by the optimization occurs when the physical requirements of the system require a spacing of the dipoles that is larger than 0.25 wavelength, otherwise a non-adaptive system seems to give better results.

3.5 Non-Ideal Crossed Dipoles With Transferred Power Optimization

The previous section shows that optimizing the circular polarization of the transmit antenna is generally insufficient to increase the transferred power in a communication system. In this section, the method of determining the effectiveness of a solution was modified to maximize the transferred power in the chosen direction. The communication

system includes a pair of crossed dipoles with minimum separation and the isotropic receiver with circular polarization at the optimization point (see Fig. 2.3). Using this setup the MATLAB script was run for several receive points with the results shown in Table 3.3. The first optimization had $\theta = 0°$ and $\phi = 0°$ as the receive point, and it produced circular polarization, as shown by the final inverse axial ratio, in the direction perpendicular to the plane containing the crossed dipoles. After this first optimization the second dipole's magnitude and phase were used as a starting point for the remaining

Table 3.3: Revised Optimizer Results for Minimum Dipole Spacing

θ (deg)	ϕ (deg)	Initial Inverse Axial Ratio	Initial Radiated Power (dBi)	Initial Power Transferred (dBi)	Final Inverse Axial Ratio	Final Radiated Power (dBi)	Optimized Power Transferred (dBi)	Increase Resulting From Optimization (dB)
0	0	0.939	2.18	2.18	1.00	2.18	2.18	0.00
10	0	0.977	2.08	2.08	0.955	2.09	2.08	0.00
20	0	0.911	1.80	1.79	0.831	1.84	1.80	0.01
30	0	0.810	1.37	1.32	0.657	1.55	1.37	0.05
40	0	0.686	0.85	0.70	0.471	1.38	0.85	0.15
50	0	0.549	0.32	-0.03	0.302	1.41	0.32	0.35
60	0	0.408	-0.16	-0.86	0.167	1.64	-0.16	0.70
70	0	0.269	-0.52	-1.77	0.072	1.90	-0.52	1.25
80	0	0.133	-0.75	-2.75	0.018	2.11	-0.75	2.00
10	45	0.986	2.08	2.08	0.970	2.08	2.08	0.00
20	45	0.943	1.79	1.78	0.883	1.81	1.79	0.01
30	45	0.873	1.31	1.29	0.750	1.41	1.32	0.03
40	45	0.777	0.69	0.62	0.587	0.99	0.71	0.09
50	45	0.657	-0.04	-0.22	0.414	0.69	0.00	0.22
60	45	0.516	-0.80	-1.23	0.251	0.61	-0.72	0.51
70	45	0.356	-1.51	-2.39	0.117	0.74	-1.37	1.02
80	45	0.183	-2.04	-3.73	0.030	0.94	-1.82	1.91
10	90	0.977	2.08	2.08	0.956	2.09	2.08	0.00
20	90	0.911	1.80	1.79	0.830	1.84	1.80	0.01
30	90	0.811	1.37	1.32	0.658	1.55	1.37	0.05
40	90	0.686	0.85	0.70	0.471	1.38	0.85	0.15
50	90	0.549	0.32	-0.03	0.302	1.42	0.32	0.35
60	90	0.408	-0.16	-0.86	0.167	1.63	-0.16	0.70
70	90	0.269	-0.52	-1.77	0.072	1.90	-0.52	1.25
80	90	0.133	-0.75	-2.75	0.017	2.11	-0.75	2.00

receive points considered. In Table 3.3 the radiated power is the power transferred between the dipoles and the optimization point without considering the polarization of the wave, or it is the power radiated in the chosen direction. The power transferred, in Table 3.3, is the radiation pattern power plus the polarization factor found with equation (1.5). It represents the gain in the link over an isotropic point source system. The final column in Table 3.3 is the change in transferred power between the non-optimized results, and the post-optimization results. This number indicates increase in power due to the optimization. The data indicates that the power transferred increased in every case, and is due to a decrease in polarization efficiency and an increase in the power radiated in the chosen direction. To understand the gain resulting from the optimization, Fig. 3.10
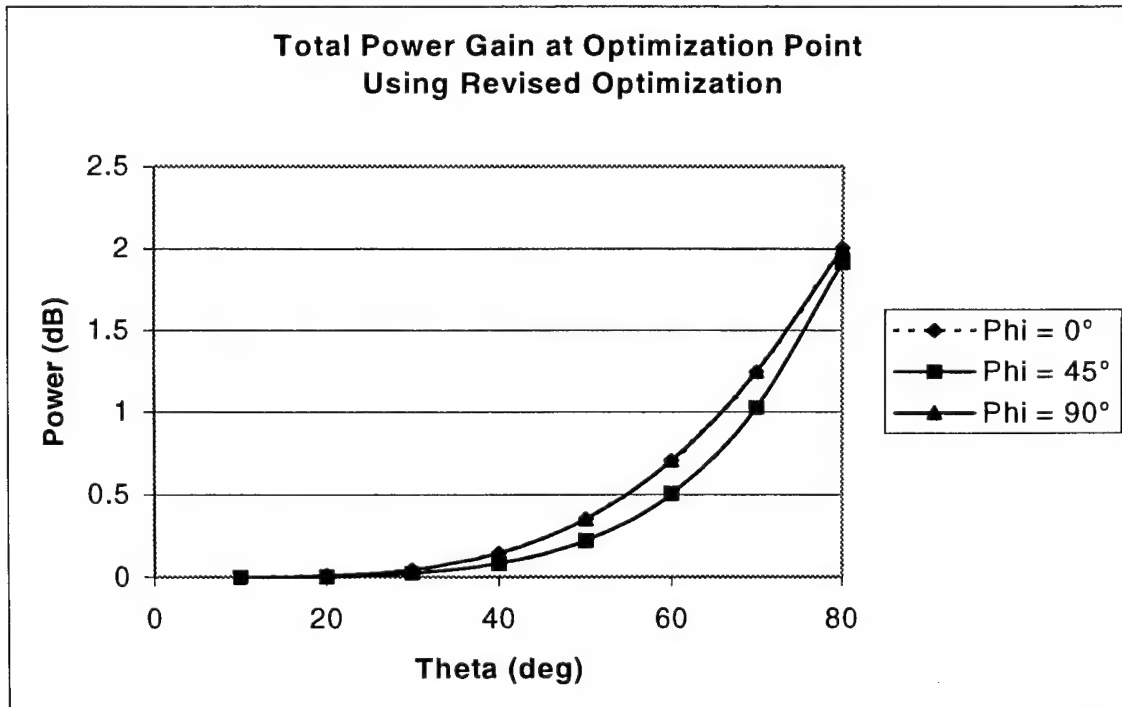
Fig. 3.10: Total improvement in gain using revised optimization.

shows a plot of the total gain vs. the angle θ. In this figure, the φ = 0° and φ = 90°

curves are nearly identical and appear to be superimposed. The greatest benefits from

this optimization are as the angle θ increases or where the losses are initially the greatest.

The antenna pattern for the receive point with the largest improvement is plotted in Fig.

3.11. The increase in gain after optimization occurs due to the movement of the nulls

away from the direction of the optimization point (see Fig. 3.11). This movement of the

nulls increases the radiation pattern power in the desired direction, and thus increases the

total power transferred. At larger angles of θ the increase in power transferred is due to

the larger loss in the radiation pattern at those angles in the initial condition. The

increases are not without a loss in polarization efficiency, as the inverse axial ratio

always decreases. The data taken for crossed dipoles with minimum separation indicates

that an increase in gain of up to 1.9 – 2.0 dB is possible depending on the receive point.

This optimization for transferred power holds promise as an effective way to increase the

View φ = 0°   View φ = 23°
View θ = 80°   View θ = 82°
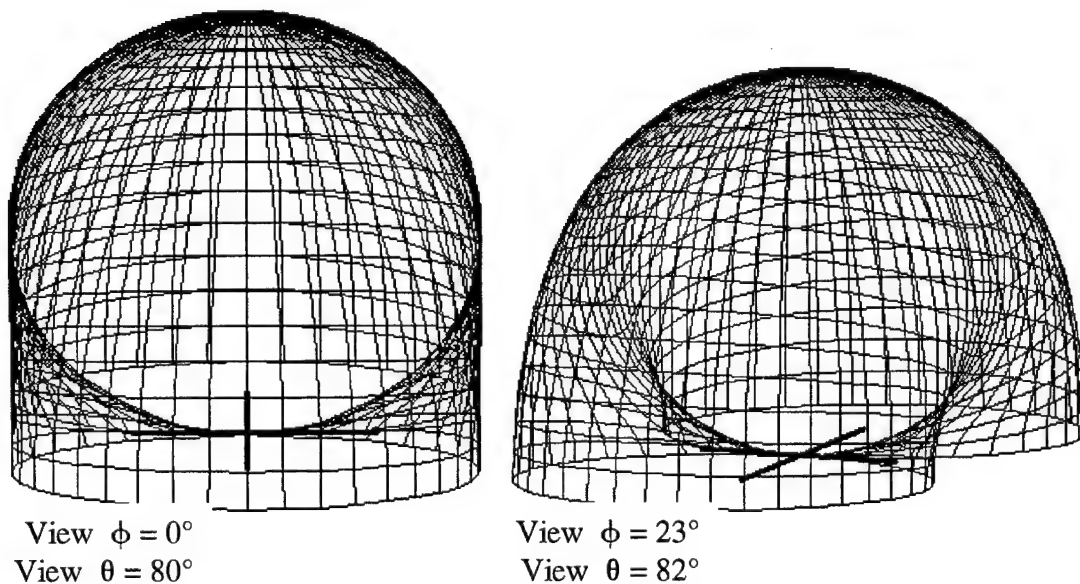
Fig. 3.11: Antenna pattern for θ = 80° and φ = 0° using transferred power optimization.

gain in a desired direction by adjusting only the magnitude and phase of one dipole. This project allows the magnitude of the second dipole be an arbitrary any value for simplicity in the optimization, but the ratio of the magnitudes between the two dipoles is the important factor in adjusting the antenna pattern and polarization. To implement this system a variable phase shifter on the second dipole and a variable power divider between the two dipoles would be needed.

An extension of the results found using a single pair of crossed dipole would be to incorporate the crossed dipoles into an array. The phasing between the array elements may be optimized to receive power from a particular direction. This array directionality could then be combined with an optimization for each element as a pair of crossed dipoles, with the resulting increase in total gain. Overall, the proposed optimization yields significant increases in the gain of a crossed dipole system at those angles where the gain is the lowest. This increase could allow improvements in a communication system, as the simple adjustments to phase and magnitude are implemented.

Another possible use of this optimization would be with a more directive antenna such as a Yagi or a helix. Using a pair of Yagi antennas the polarization would be similar to the crossed dipoles, but the antenna pattern is much more directive. This difference in antenna pattern would also limit the ability of the optimizer to increase the power transferred in any direction of propagation due to a limited ability to change the power radiated in a particular direction. The helix antenna also has limitations when used with the developed optimization. It is also highly directive and not easily adjusted to increase the power radiated in a particular direction. Also, the geometry of the helix does not lend

itself to polarization adjustment. Therefore, highly directive antennas may not lend themselves to optimization.

3.6 Crossed Dipoles as Transmit and Receive Antennas

To further improve the optimizer's ability to increase the total power transferred in a communications link, two pairs of crossed dipoles were considered with one as the transmitter and one as the receiver. The initial power transferred for the two pairs of dipoles was determined when both fed to produce circular polarization in the direction perpendicular to the dipoles. For the first set of simulations, the transmitter pair of dipoles was optimized and the receive pair maintained its circular polarization. The physical configuration of this setup is shown in Fig. 3.12 with $\theta = 45°$ and $\phi = 0°$ as the direction of propagation relative to the transmitter pair of dipoles, and $\theta = -45°$ and $\phi = 0°$ as the direction of propagation relative to the receiver pair of dipoles.
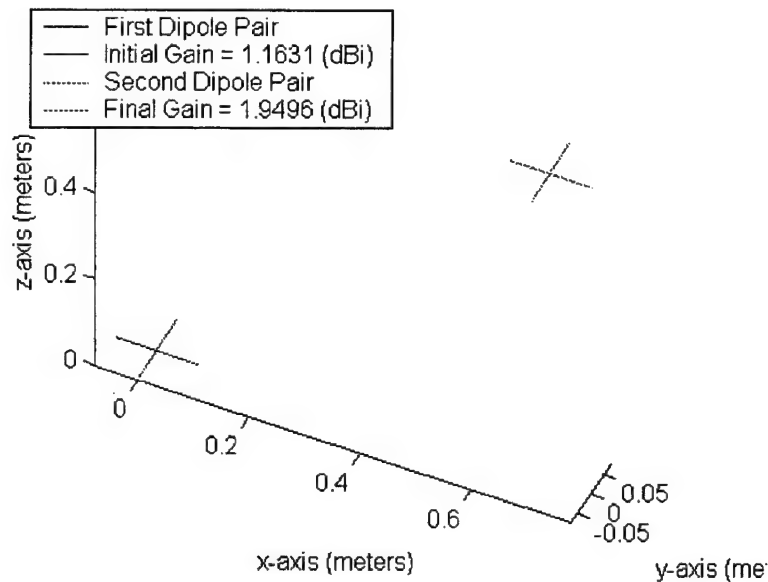
Fig. 3.12: Dual crossed dipoles with only one optimized in $\theta = \pm 45°$ and $\phi = 0°$ direction.

Using the two pairs of crossed dipoles it is possible to setup any direction of propagation relative to the transmit pair and to the receive pairs. Various directions of propagations were simulated with the results shown in Table 3.4. From these simulations the improvement over the previously considered isotropic receiver is evident, especially at the larger angles of θ. For example, at $\theta = 80°$ and $\phi = 0°$ the power transferred after optimization is 1.36 dBi where the previous result from Table 3.3 has a power transferred of -0.75 dBi. The greatest advantage of the two pairs of dipoles is found in the directivity of the second pair of dipoles and yields the increases in power transferred. In general, the optimization of just the transmitter pair of dipoles yields an increase in gain over the single pair optimization. It is also interesting to note that the optimization tends to turn off the dipole that is parallel to the direction of propagation for large angles of θ.

To further study the two pairs of crossed dipoles, the optimization was allowed to adjust both transmit and receive dipole pairs. The geometry is specified in the same way

Table 3.4: Transferred Power Optimization for Two Pairs of Dipoles, One Pair Optimized

Direction of Propagation Relative to the Transmit Pair		Direction of Propagation Relative to the Receive Pair		Power Transferred		Transmit Pair Final Parameters			Receive Pair Final Parameters		
θ (deg)	ϕ (deg)	θ (deg)	ϕ (deg)	Initial (dBi)	Final (dBi)	Radiated Power (dBi)	Inverse Axial Ratio	Tilt (deg)	Radiated Power (dBi)	Inverse Axial Ratio	Tilt (deg)
0	0	0	0	4.37	4.37	2.18	0.939	-45.1	2.18	0.939	-45.0
0	0	0	0	4.37	4.37	2.18	0.998	-78.6	2.18	1.000	-1.4
45	0	-45	0	1.16	1.95	1.83	0.237	-89.5	0.58	0.618	88.6
80	0	-80	0	-1.50	1.36	2.18	0.002	90.0	-0.75	0.133	89.5
20	45	-20	0	3.60	3.61	1.83	0.804	89.2	1.80	0.911	88.4
45	45	-45	0	1.00	1.55	1.25	0.310	89.5	0.58	0.618	88.6
60	45	-60	0	-0.81	0.67	1.19	0.102	89.7	-0.16	0.408	88.8
80	45	-80	0	-2.53	0.24	1.06	0.004	90.0	-0.75	0.133	89.5

as shown in Fig. 3.12, with the direction of propagation being set relative to each pair of dipoles. Fig. 3.13 shows a result of the optimization for both pairs of crossed dipoles. The results of several simulations where both dipoles were optimized are shown in Table 3.5. Note that in several cases the power transferred is the maximum possible for a pair of dipoles. For values of θ close to $0°$ the optimization tends towards an exact
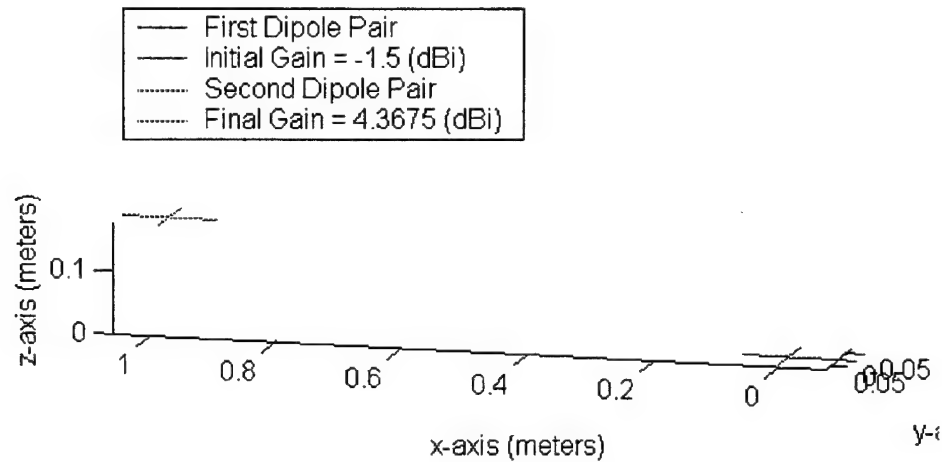
Fig. 3.13: Dual crossed dipoles with both optimized in $\theta = \pm80°$ and $\phi = 0°$ direction.

Table 3.5: Transferred Power Using Two Pairs of Dipoles With Both Optimized

Direction of Propagation Relative to the Transmit Pair		Direction of Propagation Relative to the Receive Pair		Power Transferred		Transmit Pair Final Parameters			Receive Pair Final Parameters		
θ (deg)	ϕ (deg)	θ (deg)	ϕ (deg)	Initial (dBi)	Final (dBi)	Radiated Power (dBi)	Inverse Axial Ratio	Tilt (deg)	Radiated Power (dBi)	Inverse Axial Ratio	Tilt (deg)
0	0	0	0	4.37	4.37	2.18	0.999	-45.0	2.18	1.000	-45.0
40	0	-40	0	1.70	4.37	2.18	0.000	-90.0	2.18	0.000	-90.0
80	0	-80	0	-1.50	4.37	2.18	0.000	90.0	2.18	0.000	90.0
70	45	0	45	0.06	0.85	0.77	0.031	83.8	2.18	0.138	45.3
70	90	0	0	0.41	4.37	2.18	0.000	90.0	2.18	0.000	-89.9
80	45	0	0	-1.35	3.25	1.06	0.000	90.0	2.18	0.003	-89.9

match of the polarization between transmit and receive antennas, and it is usually close to circular polarization. As the angle θ increases the optimization changes and tends to push towards a linearly polarized wave. This is intuitive for $\phi = 0°$ and $\phi = 90°$ as the dipoles parallel to the direction of propagation tend to be turned off, and the power transferred is the same as if there were only a single dipole as both the transmitter and the receiver. This tendency towards linear polarization holds true for angles of $\phi = 45°$, but both dipoles in the pair contribute part of the signal. The optimization also takes significantly longer for angles of $\phi = 45°$ than other angles, because the best solution adjusts both the magnitude and the phase of the second dipole, where the other angles of ϕ considered depend primarily on a magnitude adjustment.

In conclusion, the optimizations of both transmit and receive antennas using pairs of crossed dipoles always increases the power transferred between the two. In many cases the optimization tends to use linear polarization especially at large angles of θ. The ability to optimize at both ends of a communication system may pose formidable challenges from a controls system standpoint, but the optimization at only one end using the transmitter dipole pair indicates that some improvement may be easily implemented on one end of a communication system. Additional simulations and an experimental setup would be in order to further understand the optimizations ability to increase power transferred between two pairs of crossed dipoles.

Chapter 4

Conclusions and Recommendations

4.1 Conclusions

In general, the ability to generate the desired circular polarization with a pair of crossed dipoles was established using the selected optimization method. The optimizing function used the sense, the axial ratio, and the radiated power in a user defined optimization direction by adjusting the amplitude and phase of one of the dipoles. This correction of the polarization eliminates the loss caused by the polarization loss factor (see equation (1.5)). Although the optimization is almost always able to achieve the desired circular polarization in the optimization direction, the change in the radiated power in that same direction may offset or decrease the total gain. To overcome this effect, the optimization was changed to consider the transferred power for determining the efficiency of a solution.

For dipoles having a minimum separation, the polarization optimizer is able to achieve minor improvements for angles of $\theta < 15°$. For all other angles, the loss of power in the direction of optimization causes a greater loss than the non-optimized setup. Similar results are found for the cases containing a ground plane, where the optimization does not improve the total gain, even though it does reduce the polarization loss.

The cases where the polarization optimization improves the total power occur when the spacing between the crossed dipoles is increased beyond 0.2 wavelength. At 0.2 wavelength, the combination of the polarization correction and some increases in the radiated power in the optimization direction yields a total gain for many angles of

optimization. The largest gains are found when $\phi = 45°$ and $25° < \theta < 55°$, and in values up to 0.04 dB.

The simulations with a spacing of 0.5 wavelength gave even larger gains of up to 17.61 dB. This increase in gain was primarily due to the increase in the polarization mismatch and the ability of the optimizer to correct for the errors. The largest gains were once again seen in the $\phi = 45°$ optimization direction. Additional spacings between dipoles were considered with gain increasing after optimization when the polarization error was large.

The general failure of the polarization loss optimization prompted a revised optimization scheme based on the total power transferred. The results are promising for a dipole pair with minimum separation where the total power transferred is always increased by the optimization for angles of $\theta < 80°$, with the largest gains occurring as θ increases, or as the non-optimize gain decreases. This revised optimization holds great promise as a method to increase the gain of a communication system using an amplitude and phase adjustment. This final setup also indicates that it is not beneficial to optimize to reduce the polarization loss, but an increase in polarization loss yields a larger total gain in the chosen direction of optimization.

The optimization for total power transferred was extended to consider pairs of crossed dipoles at each end of the communication system. When only the transmitter pair was optimized, the additional directivity of the receiver increases the power transferred by up to 2.1 dB. The optimization of both the transmitter and the receiver further improved the power transferred up to the limits of the dipoles, but the optimization tends to use a linearly polarized wave.

4.2 Recommendations for Future Work

1. An area of consideration could be a look at adjusting the phase or amplitude only of the second dipole to attempt to increase the transferred power. From the results in this project it appears that when θ is about 45° the correction involves only a phase shift, and the correction when θ is 0° or 90° is mostly accomplished by adjusting the amplitude of the second dipole.

2. Using the results from this project, an experimental setup would be in order. It would require a method of adjusting the amplitude and phase of one dipole and allowing the effectiveness of the solution to be measured in a desired direction. These controls and measurements would then need to be available to the computer system running the optimization algorithm. The results should be approximately the same as those found in the simulations done with this project.

3. Finally, it would also be interesting to investigate the possibility of adjusting the response of antennas with circular polarization, such as a helix. An investigation of the ability of an optimization technique to adjust the response of such antennas to increase the transferred power in a chosen optimization direction.

References

[1] C. A. Balanis, *Antenna Theory: Analysis and Design.* New York: John Wiley & Sons, 2 ed., 1997.

[2] J. D. Kraus and D. A. Fleisch, *Electromagnetics: with Applications.* Boston: McGraw-Hill, 5 ed., 1999.

[3] C. W. Harrison Jr. and R. King, "The receiving antenna in a plane-polarized field of arbitrary orientation," *Proceedings of the I.R.E.*, vol. 32, pp. 35-49, Jan. 1944.

[4] W. Sichak and S. Milazzo, "Antennas for circular polarization," *Proceedings of the I.R.E.*, vol. 36, pp. 997-1002, Aug. 1948.

[5] Y.-C. Yeh, "The received power of a receiving antenna and the criteria for its design," *Proceedings of the I.R.E.*, vol. 37, pp. 155-158, Feb. 1948.

[6] G. Sinclair, "The transmission and reception of elliptically polarized waves," *Proceedings of the I.R.E.*, vol. 38, pp.148-151, Feb. 1950.

[7] M. G. Morgan and W. R. Evens, Jr., "Synthesis and analysis of elliptic polarization loci in terms of space-quadrature sinusoidal components," *Proceedings of the I.R.E.*, vol. 39, pp. 552-556, May 1951.

[8] R. T. Compton Jr., *Adaptive Antennas: Concepts and Performance.* New Jersey: Prentice Hall, 1988.

[9] V. H. Rumsey, "Transmission between elliptically polarized antennas," *Proceedings of the I.R.E.*, vol. 39, pp. 535-540, May 1951.

[10] G. A. Deschamps, "Geometrical representation of the polarization of a plane electromagnetic wave," *Proceedings of the I.R.E.*, vol. 39, pp. 540-544, May 1951.

[11] M. L. Kales, "Elliptically polarized waves and antennas," *Proceedings of the I.R.E.*, vol. 39, pp. 544-549, May 1951.

[12] E. F. Bolinder, "Geometric analysis of partially polarized electromagnetic waves," *IEEE Transactions on Antennas and Propagation*, vol. AP-15, pp. 37-40, Jan. 1967.

[13] S. J. Dudzinsky Jr., "Polarization discrimination for satellite communications," *Proceedings IEEE*, vol. 57, pp. 2179-2180, Dec. 1969.

[14] T. S. Chu, "Restoring the orthogonality of two polarizations in radio communication systems, II," *Bell System Technical Journal*, vol. 52, pp. 319-327, Mar. 1973.

[15] R. E. Marshall and C. W. Bostian, "An adaptive polarization correction scheme using circular polarization," *IEEE International Antennas and Propagation Society Symposium, Atlanta, GA*, pp. 395-397, June 1974.

[16] F. E. Nathanson, "Adaptive circular polarization," *IEEE International Radar Conference, Arlington, VA*, pp. 221-225, Apr. 1975.

[17] W. H. Kummer and E. S. Gillespie, "Antenna measurements – 1978," *Proceedings of the IEEE*, vol. 66, pp. 483-507, Apr. 1978.

[18] R. T. Compton, "On the performance of a polarization sensitive adaptive array," *IEEE Transactions on Antennas and Propagation*, vol. AP-29, pp. 718-725, Sept. 1981.

[19] D. M. Pozar and S. Targonski, "Axial ratio of circularly polarized antennas with amplitude and phase errors," *IEEE Antennas and Propagation Magazine*, vol. 32, pp. 45-46, Oct. 1990.

[20] S. V. Parekh, "Simple formulae for circular-polarization axial ratio calculations," *IEEE Antennas and Propagation Magazine*, vol. 33, pp. 30-32, Feb. 1991.

[21] D. M. Pozar, "Scanning characteristics of infinite arrays of printed antenna subarrays," *IEEE Transactions on Antennas and Propagation*, vol. 40, pp. 666-674, June 1992.

[22] C.-Y. Huang, J.-Y. Wu, and K.-L. Wong, "Cross-slot-coupled microstrip antenna and dielectric resonator antenna for circular polarization," *IEEE transactions on Antennas and Propagation*, vol. 47, pp. 605-609, Apr. 1999.

[23] E. L. Mokole, A. K. Choudhury, and S. N. Samaddar, "Transient radiation from thin, half-wave, orthogonal dipoles," *Radio Science*, vol. 33, pp. 219-229, Mar.-Apr. 1998.

[24] E. E. Altshuler, "Design of a vehicular antenna for GPS/IRIDIUM using a genetic algorithm," *IEEE Transactions on Antennas and Propagation*, vol. 48, pp. 968-972, June 2000.

[25] M. Tanaka, "Polarization-changeable phased array," *IEEE Antennas and Propagation Society International Symposium, 1999*, vol. 4, pp. 2322-2325, July 1999.

[26] G. J. Burke and A. J. Poggio, *Numerical Electromagnetics Code (NEC2) User's Manual*, Lawrence Livermore Lab., Jan. 1981.

[27] Y. C. Chung, February – March 2001, Private Communication.

APPENDICES

APPENDIX A. MATLAB CODE TO OPTIMIZE CROSSED DIPOLES

MATLAB FILE 'Griffin_t.m'

(Note the "→" symbol is used to represent the continuation of a line to the next.)
```
%
% Griffin_t.m
%
% Author: Brian Griffin
% Date: Feb 2001
%
% Purpose: The MATLAB file will use an optimization algorithm to control a
% pair of cross dipoles.
%


clear
format long;

global theta phi
global axial_ratio tilt sense
global wire_radius separation pos_x neg_x frequency filename wire_height ground_flag
global count listx1 listx2 listAR power desired_sense

% Variables
frequency = 1e9;
filename = 'NEC_IN';
wire_radius = 0.001;   %radius of the wire in meters
wire_height = 0.0;      %height of the dipoles in wavelengths
ground_flag = 0;        %set to one for a ground plane set to zero for no ground plane
fntsz=12;            %set the font size
iterations = 200;       %max number of iterations of optimization to try
i_mult = 0;

%input box to set the point of optimization
prompt={'Enter phi for the optimization point (in degrees):','Enter theta for the
→optimization point (in degrees):','Input the desired sense (Left or Right):'};
def={'0','40','left'};
dlgTitle='Set the Optimization Point (Remember the crossed dipoles are in the xy plane)';
lineNo=[1 40];
answer=inputdlg(prompt,dlgTitle,lineNo,def);

% Point to determine Axial Ratio at (remember the dipoles are in the xy plane)
theta = str2num(answer{2});
phi = str2num(answer{1});


% Crossed Dipoles
```

```
% use half wavelength dipoles
wavelength = 3e8 / frequency;
length = wavelength * 0.5;
pos_x = length/2;
neg_x = - pos_x;
wire_height = wire_height*wavelength;

%determine the separation required to keep the two dipoles out of contact
separation = 1.2*wavelength;%2*wire_radius + wire_radius;     %distance to keep the
→dipoles out of contact

frequency = frequency / 1e6;        %put the frequency in MHz

% Control the phase and magnitude of only one dipole
% phase (j term) go from -1 to 1

%starting point variables
mag = 0.0;      %starting real part
if strncmpi(answer(3), 'LEFT',4)
   if theta > 90
      phase = -1.0; %imaginary part of the input
   else
      phase = 1.0;     %imaginary part of the input
   end
elseif strncmpi(answer(3), 'RIGHT',5)
   if theta > 90
      phase = 1.0; %imaginary part of the input
   else
      phase = -1.0;   %imaginary part of the input
   end
else
   ['Please try again with a sense of left or right only']
   return
end
desired_sense = answer(3);
%for values that will not reverse during optimization
%phase = -phase;
%end of modification


%beginning of the loop to do multiple points
%for i_mult=50:-10:0
%theta = i_mult
%end of the start of the multiple point loop
```

```
%Run the code once to get the starting Axial Ratio and Tilt
NEC_Input(mag, phase);
!shor_ver
fid=fopen('Polar','r');    %Open the output file
temp = fscanf(fid,'%f');
fclose(fid);
axial_ratio_initial = temp(1);    %get the axial_ratio
tilt_initial = temp(2);           %get the tilt in degrees


%call the optimizer to run the NEC several times and determine a best solution for AR =
→1
count = 1;    %setup the counter to gather data at each iteration
options = optimset('Display','iter','MaxIter',iterations,'TolFun',1e-4,'TolX',1e-4);

x = fminsearch(@AR_optimize, [mag;phase],options);

%get the final axial ratio tilt and sense
AR_optimize(x);

% produce an output file that contains the antenna pattern
nec_input_final(x(1),x(2));
!shor_ver

%determine the optimized result as expected
mag = abs(x(1) + j* x(2));
phase = (180/pi)*angle(x(1) + j* x(2));

%first dipole for display
ax = [pos_x neg_x];
ay = [0 0];
az = [0 0];

%second dipole for display
by = [pos_x neg_x];
bx = [0 0];
bz = [separation separation];

%optimization point
r = 2;  %distance r (meters) to the optimization point

%convert theta and phi to radians
theta = (pi/180)*theta;
phi = (pi/180)*phi;
```

```
%locate the optimization point in xyz coordinates
ox = r * sin(theta) * cos(phi);
oy = r * sin(theta) * sin(phi);
oz = r * cos(theta);

%plot the dipoles and the optimization point
temp = figure(i_mult+1);
clf(temp)
set(axes,'FontSize',fntsz,'xlim',[0 20],'ylim',[4 40],'box','on')

plot3(ax,ay,az,'-',bx,by,bz,'r-',ox,oy,oz,'k*');
xlabel('x-axis (meters)')
ylabel('y-axis (meters)')
zlabel('z-axis (meters)')

%convert back to degrees
theta = (180/pi)*theta;
phi = (180/pi)*phi;

%set the view point
view(25+phi, 90-theta);

%optimization point text
ob_text_phi = ['Phi = ' num2str(phi) ' (deg)'];
ob_text_theta = ['Theta = ' num2str(theta) ' (deg)'];

%display the results in the legend
disp_AR_int = ['Initial Axial Ratio = ' num2str(axial_ratio_initial)];
disp_tilt_int = ['Initial Tilt = ' num2str(tilt_initial) ' (deg)'];
disp_AR = ['Final Axial Ratio = ' num2str(axial_ratio)];
%disp_tilt = ['Final Tilt = ' num2str(tilt) ' (deg)'];
disp_sense = ['Final Sense = ' num2str(sense)];
disp_power = ['Gain at Optimization point = ' num2str(power)];

%display the legend
legend('First Dipole','Second Dipole','Optimization Point',ob_text_phi,ob_text_theta,' ',
→disp_AR_int, disp_tilt_int, disp_AR, disp_sense,disp_power,2);


%display the title with the results used to drive the second dipole and achieve the desired
→results
disp_title = ['Result: Y-Axis Dipole Driven with Magnitude = ' num2str(mag) ' and Phase
→= ' num2str(phase) ' (deg)'];
title(disp_title);
```

axis equal;

%end of the loop to do multiple points
%end

%display the axial ratio as the optimization takes place
temp1 = figure(3);
clf(temp1)
set(axes,'FontSize',fntsz,'xlim',[0 20],'ylim',[4 40],'box','on')
plot(listAR);
title('Axial Ratio at Each Iteration');
xlabel('Iteration number');
ylabel('Axial Ratio');

%cleanup the extra files from the NEC output
!del fort.8
%!del NEC_OUT
%!del power_gsin

%beep when finished
beep

MATLAB FILE 'AR_optimize.m'

function test = AR_optimize(x)
global axial_ratio tilt sense
global count listx1 listx2 listAR power desired_sense
c1 = 1;   %Axial ratio cost
c2 = 0.001;   %power at the point cost
c3 = 100;   %wrong sense of rotation

mag = x(1);
phase = x(2);
listx1(count) = x(1);
listx2(count) = x(2);

%create the Nec input file
NEC_Input(mag, phase);

%excute the NEC code for the input
!shor_ver

```
fid=fopen('Polar','r');    %Open the output file
temp = fscanf(fid,'%f');
sense = fscanf(fid,'%s');
fclose(fid);
fid=fopen('Power_gsin','r');    %open the power file
power = fscanf(fid,'%f');
fclose(fid);

axial_ratio = temp(1);      %get the axial_ratio
listAR(count) = temp(1);    %store each iteration's AR
tilt = temp(2);             %get the tilt in degrees

test_sense = 1 - strncmpi(desired_sense,sense,4);

test = c1*(1 - axial_ratio) + c2*(2.16-power) + c3*test_sense;

count = count + 1;          %increment the function counter
```

MATLAB FILE 'NEC_input.m'

```
%
% NEC_Input.m
%
% NEC input creation function
%
% Inputs:
% magnitude of the second dipole - mag
% phase of the second dipole - phase
% frequency of operation - frequency
%

function NEC_Input(mag, phase)

global theta phi wire_radius separation pos_x neg_x frequency filename wire_height
→ground_flag
% Creation of the Input file for MATLAB
% Patterned after a file created by: You Chung Chung



fid=fopen(filename,'wt');    %Open the output file
```

```
% file comments
fprintf(fid,'CM MATLAB generated file to adjust a set of crossed\n');
fprintf(fid,'CM dipoles to adjust their polarization to achieve\n');
fprintf(fid,'CM the best gain for a given magnitude and phase on\n');
fprintf(fid,'CM one of the dipoles.  A Helix will be used to drive\n');
fprintf(fid,'CM the dipoles from different locations.\n');
fprintf(fid,'CE\n');

% first dipole
fprintf(fid,'GW 1 11 %6.5f 0.00000 %6.5f %6.5f 0.00000 %6.5f
→%7.6f\n',neg_x,wire_height,pos_x,wire_height,wire_radius);

% second dipole  (Look to see if this needs to be up from the first dipole)
fprintf(fid,'GW 2 11 0.00000 %6.5f %6.5f 0.00000 %6.5f %6.5f
→%7.6f\n',neg_x,wire_height+separation,pos_x,wire_height+separation,wire_radius);

% end of geometry

fprintf(fid,'GS 0 0 1\n');
fprintf(fid,'GE 0\n');
if ground_flag
    fprintf(fid,'GN 1\n');
end

%excitation of the dipoles
fprintf(fid,'EX  0   1   6  00   1.00000   0.00000\n'); %excite the first dipole

fprintf(fid,'EX  0   2   6  00   %6.5f   %6.5f\n',mag,phase); %excite the second dipole

%frequency line

fprintf(fid,'FR 0 1 0 0 %6i 0\n',frequency); %frequency output

%calculation field
fprintf(fid,'RP 0 1 1 1501 %6.5f %6.5f 1 1\n',theta,phi);  %calculation output


%end of file
fprintf(fid,'EN\n');

fclose(fid);
```

MATLAB FILE 'NEC_Input_final.m'

```
%
% NEC_Input_final.m
%
% NEC input creation function
%
% Inputs:
% magnitude of the second dipole - mag
% phase of the second dipole - phase
% frequency of operation - frequency
%

function NEC_Input_final(mag, phase)

global wire_radius separation pos_x neg_x frequency filename phi wire_height
ground_flag
% Creation of the Input file for MATLAB
% Patterned after a file created by: You Chung Chung


fid=fopen(filename,'wt');    %Open the output file

% file comments
fprintf(fid,'CM MATLAB generated file to adjust a set of crossed\n');
fprintf(fid,'CM dipoles to adjust their polarization to achieve\n');
fprintf(fid,'CM the best gain for a given magnitude and phase on\n');
fprintf(fid,'CM one of the dipoles. \n');
fprintf(fid,'CE\n');

% first dipole
fprintf(fid,'GW 1 11 %6.5f 0.00000 %6.5f %6.5f 0.00000 %6.5f
→%7.6f\n',neg_x,wire_height,pos_x,wire_height,wire_radius);

% second dipole  (Look to see if this needs to be up from the first dipole)
fprintf(fid,'GW 2 11 0.00000 %6.5f %6.5f 0.00000 %6.5f %6.5f
→%7.6f\n',neg_x,wire_height+seperation,pos_x,wire_height+seperation,wire_radius);

% end of geometry

fprintf(fid,'GS 0 0 1\n');
fprintf(fid,'GE 0\n');
if ground_flag
   fprintf(fid,'GN 1\n');
end
```

%excitation of the dipoles
fprintf(fid,'EX 0   1   6 00   1.00000   0.00000\n'); %excite the first dipole

fprintf(fid,'EX 0   2   6 00   %6.5f   %6.5f\n',mag,phase); %excite the second dipole

%frequency line

fprintf(fid,'FR 0 1 0 0 %6i 0\n',frequency); %frequency output

%calculation field
fprintf(fid,'RP 0 19 1 1501 0 %6.5f 5 1\n',phi); %calculation output
%fprintf(fid,'RP 0 1 360 1501 90 0 1 1\n'); %calculation output

%end of file
fprintf(fid,'EN\n');

fclose(fid);

UPDATED MATLAB FILE 'AR_optimize.m' to consider total transferred power.

```
function test = AR_optimize(x)
global axial_ratio tilt sense
global count listx1 listx2 listAR power desired_sense

mag = x(1);
phase = x(2);
listx1(count) = x(1);
listx2(count) = x(2);


%create the Nec input file
NEC_Input(mag, phase);

%excute the NEC code for the input
!shor_ver

fid=fopen('Polar','r');    %Open the output file
temp = fscanf(fid,'%f');
sense = fscanf(fid,'%s');
fclose(fid);
fid=fopen('Power_gsin','r');    %open the power file
```

```
power = fscanf(fid,'%f');
fclose(fid);

axial_ratio = temp(1);      %get the axial_ratio
listAR(count) = temp(1);    %store each iteration's AR
tilt = temp(2);             %get the tilt in degrees

if strncmpi(desired_sense,sense,4)     %check for the proper sense
    axial_ratio = axial_ratio;      %proper sense
else
    axial_ratio = - axial_ratio;    %wrong sense
end

mm = (pi/2-2*atan(axial_ratio));       %match angle

match_f = (cos(mm/2))^2;               %match factor

test =  10 +10*log10(match_f) + power; %function to maximize the 100 is to keep the
→power values positive

test = 1/test;          %set it up as a min.

count = count + 1;         %increment the function counter
```

APPENDIX B. TABLES OF SIMULATED RESULTS

Table B.1: Ideal Dipoles, No Ground Plane, and No Optimization

Theta (Deg)	Phi (Deg)	Pre-Opt. Gain (dBi)	Inverse Axial Ratio	Tilt Angle (Deg)	Pre-Opt. Sense	Poincaré Latitude	Match Ang. (Deg)	Pol. Error Loss (dBi)	Total Gain (dB)
0	0	2.16	0.99999	25.94	LEFT	89.999	0.001	-1.1E-10	1.09E-10
5	0	2.14	0.99428	89.6	LEFT	89.671	0.329	-3.6E-05	3.57E-05
10	0	2.07	0.9773	89.62	LEFT	88.685	1.315	-0.00057	0.000572
15	0	1.95	0.94961	89.63	LEFT	87.039	2.961	-0.0029	0.0029
20	0	1.78	0.91209	89.63	LEFT	84.735	5.265	-0.00917	0.00917
25	0	1.58	0.86589	89.64	LEFT	81.778	8.222	-0.02238	0.022378
30	0	1.35	0.81231	89.65	LEFT	78.175	11.825	-0.04633	0.046332
35	0	1.1	0.75276	89.66	LEFT	73.942	16.058	-0.08556	0.085564
40	0	0.84	0.68866	89.67	LEFT	69.107	20.893	-0.14517	0.145175
45	0	0.57	0.62133	89.69	LEFT	63.708	26.292	-0.23066	0.230664
50	0	0.31	0.55199	89.71	LEFT	57.797	32.203	-0.3476	0.347605
55	0	0.06	0.48163	89.74	LEFT	51.434	38.566	-0.5015	0.501497
60	0	-0.17	0.41104	89.77	LEFT	44.689	45.311	-0.69749	0.697487
65	0	-0.37	0.3408	89.8	LEFT	37.638	52.362	-0.94022	0.940225
70	0	-0.54	0.27123	89.83	LEFT	30.35	59.650	-1.2341	1.234104
75	0	-0.67	0.20247	89.87	LEFT	22.892	67.108	-1.5833	1.583298
80	0	-0.77	0.13448	89.91	LEFT	15.318	74.682	-1.9922	1.992203
85	0	-0.83	0.06708	89.96	LEFT	7.6753	82.325	-2.46586	2.465859
90	0	-0.85	0	-90	LINEAR	0	90.000	-3.0103	3.0103

Table B.2: Minimum Dipole Separation, No Ground Plane, and Initially Optimized

Theta (Deg)	Phi (Deg)	Pre-Opt. Gain (dBi)	Inverse Axial Ratio	Tilt Angle (Deg)	Pre-Opt. Sense	Post-Opt Gain (dBi)	Poincaré Latitude	Match Ang. (Deg)	Pol. Error Loss (dBi)	Total Gain (dB)
0	0	2.16	0.99961	63.16	LEFT	2.16	89.978	0.022	-1.7E-07	1.65E-07
5	0	2.14	0.99403	87.71	LEFT	2.14	89.657	0.343	-3.9E-05	3.89E-05
10	0	2.07	0.97705	88.8	LEFT	2.06	88.67	1.330	-0.00059	-0.009415
15	0	1.95	0.94936	89.01	LEFT	1.93	87.024	2.976	-0.00293	-0.01707
20	0	1.78	0.91184	89.09	LEFT	1.75	84.72	5.280	-0.00922	-0.020775
25	0	1.58	0.86564	89.14	LEFT	1.49	81.762	8.238	-0.02247	-0.067533
30	0	1.36	0.81206	89.17	LEFT	1.17	78.157	11.843	-0.04647	-0.143532
35	0	1.1	0.75251	89.2	LEFT	0.76	73.924	16.076	-0.08576	-0.25424
0	45	2.21	0.99997	74.41	LEFT	2.21	89.998	0.002	-9.8E-10	9.77E-10
10	45	2.11	0.9869	89.97	LEFT	2.11	89.244	0.756	-0.00019	0.000189
15	45	1.98	0.97057	89.98	LEFT	1.98	88.289	1.711	-0.00097	0.000969
20	45	1.81	0.94772	89.99	LEFT	1.79	86.925	3.0750871	-0.00313	-0.016872

Table B.3: Minimum Dipole Separation, No Ground Plane, and Not Initially Optimized

Theta (Deg)	Phi (Deg)	Pre-Opt. Gain (dBi)	Inverse Axial Ratio	Tilt Angle (Deg)	Pre-Opt. Sense	Post-Opt Gain (dBi)	Poincaré Latitude	Match Ang. (Deg)	Pol. Error Loss (dBi)	Total Gain (dB)
0	45	2.18	0.95392	-90	LEFT	2.18	87.298	2.702	-0.00241	0.002415
5	45	2.15	0.95046	-90	LEFT	2.15	87.09	2.910	-0.0028	0.002801
10	45	2.08	0.94011	-90	LEFT	2.0745	86.464	3.536	-0.00414	-0.001363
15	45	1.96	0.9229	-90	LEFT	1.9466	85.408	4.592	-0.00698	-0.006424
20	45	1.79	0.89895	-90	LEFT	1.7645	83.908	6.092	-0.01228	-0.01322
40	45	0.74	0.73886	-90	LEFT	0.39512	72.918	17.082	-0.09686	-0.248019

Table B.4: Dipole Separation 0.1 Wavelength, No Ground Plane, Not Initially Optimized

Theta (Deg)	Phi (Deg)	Pre-Opt. Gain (dBi)	Inverse Axial Ratio	Tilt Angle (Deg)	Pre-Opt. Sense	Post-Opt Gain (dBi)	Poincaré Latitude	Match Ang. (Deg)	Pol. Error Loss (dBi)	Total Gain (dB)
0	45	2.14	0.93902	-90	LEFT	2.1386	86.397	3.603	-0.00429	0.002893
15	45	1.93	0.90898	-90	LEFT	1.9164	84.54	5.460	-0.00986	-0.003738

Table B.5: Minimum Dipole Separation, Ground Plane at 0.25 Wavelengths, and Not Initially Optimized

Theta (Deg)	Phi (Deg)	Pre-Opt. Gain (dBi)	Inverse Axial Ratio	Tilt Angle (Deg)	Pre-Opt. Sense	Post-Opt Gain (dBi)	Poincaré Latitude	Match Ang. (Deg)	Pol. Error Loss (dBi)	Total Gain (dB)
0	45	7.43	0.96821	-84.43	LEFT	7.4316	88.149	1.851	-0.00113	0.002733
5	45	7.41	0.96465	-85.32	LEFT	7.4079	87.938	2.062	-0.00141	-0.000694
10	45	7.34	0.95385	-87.15	LEFT	7.3343	87.294	2.706	-0.00242	-0.003278
15	45	7.21	0.93572	-88.78	LEFT	7.2039	86.196	3.804	-0.00479	-0.001314
45	45	4.79	0.6847	88.77	LEFT	4.2359	68.799	21.201	-0.14952	-0.404583
60	45	1.73	0.48404	89.04	LEFT	-0.29293	51.658	38.342	-0.49558	-1.527353

Table B.6: Minimum Dipole Separation, Ground Plane at 0.375 Wavelengths, and Not Initially Optimized

Theta (Deg)	Phi (Deg)	Pre-Opt. Gain (dBi)	Inverse Axial Ratio	Tilt Angle (Deg)	Pre-Opt. Sense	Post-Opt Gain (dBi)	Poincaré Latitude	Match Ang. (Deg)	Pol. Error Loss (dBi)	Total Gain (dB)
0	45	3.76	0.95341	-54.55	LEFT	3.7467	87.267	2.733	-0.00247	-0.01083
40	45	5.31	0.7541	89.05	LEFT	4.9922	74.04	15.960	-0.08452	-0.23328
45	45	5.21	0.69591	88.69	LEFT	4.6764	69.669	20.331	-0.13743	-0.396166
65	45	2.43	0.41568	88.88	LEFT	-0.50379	45.143	44.857	-0.6832	-2.25059

Table B.7: Minimum Dipole Separation, Ground Plane at 0.15 Wavelengths, and Not Initially Optimized

Theta (Deg)	Phi (Deg)	Pre-Opt. Gain (dBi)	Inverse Axial Ratio	Tilt Angle (Deg)	Pre-Opt. Sense	Post-Opt Gain (dBi)	Poincaré Latitude	Match Ang. (Deg)	Pol. Error Loss (dBi)	Total Gain (dB)
0	45	8.54	0.96548	86.02	LEFT	8.5408	87.988	2.012	-0.00134	0.002139
45	45	4.47	0.68254	88.82	LEFT	3.9069	68.63	21.370	-0.15192	-0.411181

Table B.8: Dipole Separation 0.1 Wavelengths, No Ground Plane, and Not Initially Optimized

Theta (Deg)	Phi (Deg)	Pre-Opt. Gain (dBi)	Inverse Axial Ratio	Tilt Angle (Deg)	Pre-Opt. Sense	Post-Opt Gain (dBi)	Poincaré Latitude	Match Ang. (Deg)	Pol. Error Loss (dBi)	Total Gain (dB)
0	45	2.18	0.50926	90	LEFT	2.1837	53.976	36.024	-0.43647	0.440169
15	45	2.04	0.50501	90	LEFT	1.9544	53.588	36.412	-0.44607	0.360471
25	45	1.8	0.49569	90	LEFT	1.5321	52.734	37.266	-0.46763	0.199733

Table B.9: Dipole Separation 0.1 Wavelengths, No Ground Plane, and Initially Optimized

Theta (Deg)	Phi (Deg)	Pre-Opt. Gain (dBi)	Inverse Axial Ratio	Tilt Angle (Deg)	Pre-Opt. Sense	Post-Opt Gain (dBi)	Poincaré Latitude	Match Ang. (Deg)	Pol. Error Loss (dBi)	Total Gain (dB)
0	45	2.18	0.99997	-8.23	LEFT	2.18	89.998	0.002	-9.8E-10	9.77E-10
15	45	1.96	0.98687	-89.98	LEFT	1.9544	89.243	0.757	-0.00019	-0.00541
25	45	1.55	0.96136	-89.99	LEFT	1.5321	87.743	2.257	-0.00169	-0.016215

Table B.10: Dipole Separation 1.2 Wavelengths, No Ground Plane, and Not Initially Optimized

Theta (Deg)	Phi (Deg)	Pre-Opt. Gain (dBi)	Inverse Axial Ratio	Tilt Angle (Deg)	Pre-Opt. Sense	Post-Opt Gain (dBi)	Poincaré Latitude	Match Ang. (Deg)	Pol. Error Loss (dBi)	Total Gain (dB)
0	0	2.18	0.15581	-45	LEFT	2.18	17.712	72.288	-1.85674	1.856744
40	0	0.85	0.51578	64.16	LEFT	0.25	54.568	35.432	-0.42201	-0.177987
50	0	0.32	0.05451	61.33	LEFT	-1.15	6.2402	83.760	-2.56217	1.092171

Table B.11: Dipole Separation 1.2 Wavelengths, No Ground Plane, and Initially Optimized

Theta (Deg)	Phi (Deg)	Pre-Opt. Gain (dBi)	Inverse Axial Ratio	Tilt Angle (Deg)	Pre-Opt. Sense	Post-Opt Gain (dBi)	Poincaré Latitude	Match Ang. (Deg)	Pol. Error Loss (dBi)	Total Gain (dB)
0	0	2.18	0.99997	-88.85	LEFT	2.18	89.998	0.002	-9.8E-10	9.77E-10
40	0	0.85	-0.0935	55.73	RIGHT	0.25	-10.683	100.683	-3.90075	3.300746
50	0	0.32	-0.4646	73.13	RIGHT	-1.15	-49.839	139.839	-9.28554	7.815544

Table B.12: Dipole Separation 0.2 Wavelengths, No Ground Plane, and Not Initially Optimized

Theta (Deg)	Phi (Deg)	Pre-Opt. Gain (dBi)	Inverse Axial Ratio	Tilt Angle (Deg)	Pre-Opt. Sense	Post-Opt Gain (dBi)	Poincaré Latitude	Match Ang. (Deg)	Pol. Error Loss (dBi)	Total Gain (dB)
0	45	2.18	0.15795	90	LEFT	2.18	17.951	72.049	-1.84352	1.843523
5	45	2.17	0.1598	90	LEFT	2.15	18.158	71.842	-1.83215	1.812147
10	45	2.15	0.16521	90	LEFT	2.08	18.762	71.238	-1.79916	1.729165
15	45	2.1	0.17386	90	LEFT	1.95	19.726	70.274	-1.7473	1.597304
20	45	2.03	0.18519	90	LEFT	1.77	20.983	69.017	-1.68099	1.420986
25	45	1.94	0.19845	90	LEFT	1.53	22.449	67.551	-1.60566	1.195655
30	45	1.84	0.21275	90	LEFT	1.23	24.021	65.979	-1.52713	0.917128
35	45	1.7	0.22703	90	LEFT	0.86	25.582	64.418	-1.45147	0.611465
40	45	1.55	0.24012	90	LEFT	0.4	27.004	62.996	-1.38448	0.234477
45	45	1.36	0.25078	90	LEFT	-0.15	28.157	61.843	-1.33157	-0.178433
50	45	1.14	0.25767	90	LEFT	-0.82	28.898	61.102	-1.29814	-0.661858
55	45	0.89	0.25943	90	LEFT	-1.64	29.087	60.913	-1.2897	-1.2403
60	45	0.59	0.25463	90	LEFT	-2.66	28.571	61.429	-1.31282	-1.937184
0	0	2.18	0.15795	-45	LEFT	2.18	17.951	72.049	-1.84352	1.843523
5	0	2.16	0.16045	-45.17	LEFT	2.16	18.231	71.769	-1.82816	1.828162
10	0	2.08	0.16791	-45.7	LEFT	2.08	19.063	70.937	-1.78286	1.782862
15	0	1.96	0.18018	-46.6	LEFT	1.95	20.428	69.572	-1.71009	1.700088
20	0	1.8	0.19694	-47.87	LEFT	1.76	22.283	67.717	-1.61411	1.574111
30	0	1.37	0.24141	-51.72	LEFT	1.18	27.144	62.856	-1.378	1.187996
40	0	0.85	0.29127	-57.61	LEFT	0.25	32.479	57.521	-1.14361	0.543608

Table B.13: Dipole Separation 0.85 Wavelengths, No Ground Plane, and Initially Optimized

Theta (Deg)	Phi (Deg)	Pre-Opt. Gain (dBi)	Inverse Axial Ratio	Tilt Angle (Deg)	Pre-Opt. Sense	Post-Opt Gain (dBi)	Poincaré Latitude	Match Ang. (Deg)	Pol. Error Loss (dBi)	Total Gain (dB)
0	0	2.18	0.99995	15.62	LEFT	2.18	89.997	0.003	-2.7E-09	2.71E-09
20	0	1.8	0.70967	53.15	LEFT	1.76	70.724	19.276	-0.12347	0.083468
35	0	1.11	0.29457	54.69	LEFT	0.76	32.827	57.173	-1.12917	0.779172
50	0	0.32	-0.14638	62.02	RIGHT	-1.15	-16.656	106.656	-4.47708	3.007082
55	0	0.07	-0.2757	68.44	RIGHT	-2.1	-30.827	120.827	-6.1301	3.960095
60	0	-0.16	-0.35304	78.26	RIGHT	-3.25	-38.89	128.890	-7.30288	4.212876
65	0	-0.36	-0.33809	89.04	RIGHT	-4.67	-37.36	127.360	-7.06436	2.754361
85	0	-0.81	0.01192	-86.26	LEFT	-12.38	1.3659	88.634	-2.90799	-8.662007

Table B.14: Dipole Separation 0.2 Wavelengths, No Ground Plane, and Initially Optimized

Theta (Deg)	Phi (Deg)	Pre-Opt. Gain (dBi)	Inverse Axial Ratio	Tilt Angle (Deg)	Pre-Opt. Sense	Post-Opt Gain (dBi)	Poincaré Latitude	Match Ang. (Deg)	Pol. Error Loss (dBi)	Total Gain (dB)
0	45	2.18	0.99996	45.63	LEFT	2.18	89.998	0.002	-1.7E-09	1.74E-09
5	45	2.16	0.99903	1.1	LEFT	2.15	89.944	0.056	-1E-06	-0.009999
10	45	2.08	0.99621	0.28	LEFT	2.08	89.782	0.218	-1.6E-05	1.57E-05
15	45	1.95	0.99184	0.13	LEFT	1.95	89.531	0.469	-7.3E-05	7.29E-05
20	45	1.77	0.98639	0.08	LEFT	1.77	89.215	0.785	-0.0002	0.000204
25	45	1.52	0.98048	0.05	LEFT	1.53	88.871	1.129	-0.00042	0.010422
30	45	1.21	0.97489	0.04	LEFT	1.23	88.543	1.457	-0.0007	0.020702
35	45	0.83	0.97053	0.04	LEFT	0.86	88.286	1.714	-0.00097	0.030971
40	45	0.36	0.96849	0.03	LEFT	0.4	88.166	1.834	-0.00111	0.041113
45	45	-0.19	0.9701	0.04	LEFT	-0.15	88.261	1.739	-0.001	0.041
50	45	-0.86	0.97711	0.05	LEFT	-0.82	88.673	1.327	-0.00058	0.040582
55	45	-1.66	0.99197	0.15	LEFT	-1.64	89.538	0.462	-7.1E-05	0.020071
60	45	-2.61	0.98181	89.93	LEFT	-2.66	88.948	1.052	-0.00037	-0.049634
0	0	2.18	0.99996	-89.39	LEFT	2.18	89.998	0.002	-1.7E-09	1.74E-09
5	0	2.16	0.99242	70.04	LEFT	2.16	89.564	0.436	-6.3E-05	6.29E-05
10	0	2.08	0.97012	70.01	LEFT	2.08	88.262	1.738	-0.001	0.000999
15	0	1.96	0.93412	70.05	LEFT	1.95	86.098	3.902	-0.00504	-0.004964
20	0	1.8	0.88598	70.15	LEFT	1.76	83.081	6.919	-0.01584	-0.024155
30	0	1.37	0.76143	70.52	LEFT	1.18	74.573	15.427	-0.07895	-0.111054
40	0	0.85	0.61356	71.26	LEFT	0.25	63.063	26.937	-0.24222	-0.357779

Table B.15: Dipole Separation 0.35 Wavelengths, No Ground Plane, and Initially Optimized

Theta (Deg)	Phi (Deg)	Pre-Opt. Gain (dBi)	Inverse Axial Ratio	Tilt Angle (Deg)	Pre-Opt. Sense	Post-Opt Gain (dBi)	Poincaré Latitude	Match Ang. (Deg)	Pol. Error Loss (dBi)	Total Gain (dB)
0	0	2.18	0.99996	-25.3	LEFT	2.18	89.998	0.002	-1.7E-09	1.74E-09
20	0	1.8	0.84899	62.4	LEFT	1.76	80.662	9.338	-0.02887	-0.011128
40	0	0.85	0.51016	63.88	LEFT	0.25	54.058	35.942	-0.43445	-0.165547

Table B.16: Dipole Separation 0.25 Wavelengths, No Ground Plane, and Initially Optimized

Theta (Deg)	Phi (Deg)	Pre-Opt. Gain (dBi)	Inverse Axial Ratio	Tilt Angle (Deg)	Pre-Opt. Sense	Post-Opt Gain (dBi)	Poincaré Latitude	Match Ang. (Deg)	Pol. Error Loss (dBi)	Total Gain (dB)
0	0	2.18	0.99996	2.58	LEFT	2.18	89.998	0.002	-1.7E-09	1.74E-09
45	0	0.58	0.49898	68.95	LEFT	-0.38	53.037	36.963	-0.45994	-0.500058
80	0	-0.75	0.03341	82.64	LEFT	-12.38	3.8271	86.173	-2.72969	-8.900308

Table B.17: Dipole Separation 0.5 Wavelengths, No Ground Plane, and Initially Optimized

Theta (Deg)	Phi (Deg)	Pre-Opt. Gain (dBi)	Inverse Axial Ratio	Tilt Angle (Deg)	Pre-Opt. Sense	Post-Opt Gain (dBi)	Poincaré Latitude	Match Ang. (Deg)	Pol. Error Loss (dBi)	Total Gain (dB)
0	0	2.18	0.99997	-43.09	LEFT	2.18	89.998	0.002	-9.8E-10	9.77E-10
25	0	1.6	0.71497	58.25	LEFT	1.51	71.127	18.873	-0.11834	0.028337
35	0	1.12	0.50732	59.09	LEFT	0.76	53.799	36.201	-0.44083	0.080834
40	0	0.85	0.39901	59.86	LEFT	0.25	43.505	46.495	-0.7355	0.135501
45	0	0.58	0.2911	60.96	LEFT	-0.38	32.461	57.539	-1.14436	0.184356
50	0	0.32	0.18582	62.54	LEFT	-1.15	21.053	68.947	-1.67735	0.207352
55	0	0.07	0.08595	64.75	LEFT	-2.1	9.825	80.175	-2.32607	0.156069
60	0	-0.16	-0.00413	67.78	RIGHT	-3.25	-0.4733	90.473	-3.04632	-0.043679
65	0	-0.36	-0.07742	71.76	RIGHT	-4.69	-8.854	98.854	-3.73617	-0.593827
75	0	-0.65	-0.13738	81.66	RIGHT	-8.92	-15.645	105.645	-4.37511	-3.894889
0	45	2.18	0.99997	-88.14	LEFT	2.18	89.998	0.002	-9.8E-10	9.77E-10
5	45	2.16	0.99191	-0.01	LEFT	2.16	89.535	0.465	-7.2E-05	7.16E-05
10	45	2.08	0.96808	0	LEFT	2.08	88.142	1.858	-0.00114	0.001142
15	45	1.94	0.92995	0	LEFT	1.95	85.843	4.157	-0.00572	0.015718
20	45	1.74	0.87941	0	LEFT	1.77	82.657	7.343	-0.01784	0.047843
25	45	1.45	0.81833	0	LEFT	1.53	78.589	11.411	-0.04314	0.123137
30	45	1.06	0.74801	0	LEFT	1.23	73.594	16.406	-0.08933	0.259328
35	45	0.54	0.66873	0	LEFT	0.86	67.544	22.456	-0.16786	0.487863
40	45	-0.13	0.57932	0	LEFT	0.4	60.169	29.831	-0.2977	0.827699
45	45	-0.98	0.47656	0	LEFT	-0.15	50.961	39.039	-0.51411	1.344111
50	45	-2.03	0.35432	0	LEFT	-0.82	39.021	50.979	-0.88949	2.099494
55	45	-3.3	0.20164	0	LEFT	-1.64	22.801	67.199	-1.5879	3.247896
60	45	-4.7	-0.00102	0	RIGHT	-2.66	-0.1169	90.117	-3.01917	5.059169
65	45	-5.96	-0.29046	0	RIGHT	-3.95	-32.393	122.393	-6.34253	8.352525
70	45	-6.52	-0.74292	0	RIGHT	-5.63	-73.219	163.219	-16.7177	17.60766
75	45	-5.99	-0.64874	-90	RIGHT	-7.91	-65.946	155.946	-13.6232	11.70325
80	45	-4.72	-0.30792	-90	RIGHT	-11.26	-34.229	124.229	-6.60058	0.06058

Table B.18: Minimum Dipole Separation, No Ground Plane, and Revised Optimizer

θ (deg)	φ (deg)	Initial Inverse Axial Ratio	Initial Radiated Power (dBi)	Initial Total Power (dBi)	Final Inverse Axial Ratio	Final Radiated Power (dBi)	Optimized Transferred Power (dBi)	Total Gain From Optimization (dB)
0	0	0.93902	2.1837	2.1794	0.99997	2.1837	2.1837	0.0043
10	0	0.97706	2.0841	2.0836	0.95485	2.0865	2.0841	0.0005
20	0	0.91116	1.7989	1.7895	0.83088	1.8358	1.7989	0.0094
30	0	0.81048	1.3673	1.32	0.65704	1.5495	1.3674	0.0474
40	0	0.68603	0.84994	0.70189	0.4712	1.3777	0.84998	0.14809
50	0	0.54891	0.31884	-0.03472	0.30236	1.4145	0.31891	0.35363
60	0	0.40802	-0.1564	-0.86329	0.16651	1.635	-0.15633	0.70696
70	0	0.26878	-0.5227	-1.7683	0.07218	1.9048	-0.52272	1.24558
80	0	0.13308	-0.75012	-2.7515	0.01797	2.107	-0.75001	2.00149
10	45	0.98575	2.0834	2.0832	0.97019	2.0845	2.0835	0.0003
20	45	0.94326	1.7879	1.7842	0.88278	1.8057	1.7889	0.0047
30	45	0.87335	1.3134	1.2936	0.75002	1.4064	1.3186	0.025
40	45	0.77739	0.68924	0.62164	0.58701	0.99049	0.70591	0.08427
50	45	0.65739	-0.03915	-0.22088	0.4135	0.69143	0.001546	0.222426
60	45	0.51597	-0.80422	-1.2258	0.25067	0.61058	-0.72153	0.50427
70	45	0.35647	-1.5106	-2.3922	0.11662	0.74467	-1.3662	1.026
80	45	0.18291	-2.0376	-3.7318	0.03002	0.9374	-1.8199	1.9119
10	90	0.97703	2.0841	2.0836	0.9556	2.0864	2.0841	0.0005
20	90	0.91122	1.7989	1.7896	0.83018	1.8361	1.7989	0.0093
30	90	0.81065	1.3674	1.3202	0.65769	1.5487	1.3674	0.0472
40	90	0.6863	0.85004	0.70229	0.47081	1.3787	0.84999	0.1477
50	90	0.54925	0.31899	-0.03391	0.30153	1.4181	0.31893	0.35284
60	90	0.40838	-0.1562	-0.86197	0.1674	1.6296	-0.15628	0.70569
70	90	0.2691	-0.52253	-1.7665	0.07249	1.9026	-0.52263	1.24387
80	90	0.13328	-0.74985	-2.7499	0.01787	2.1079	-0.74995	1.99995

Table B.19: Transferred Power Using Two Pairs of Dipoles With Both Optimized

Direction of Propagation Relative to the Transmit Pair		Direction of Propagation Relative to the Receive Pair		Power Transferred		Transmit Pair Final Parameters			Receive Pair Final Parameters		
θ (deg)	ϕ (deg)	θ (deg)	ϕ (deg)	Initial (dBi)	Final (dBi)	Radiated Power (dBi)	Inverse Axial Ratio	Tilt (deg)	Radiated Power (dBi)	Inverse Axial Ratio	Tilt (deg)
0	0	0	0	4.37	4.37	2.18	0.999	-45.0	2.18	1.000	-45.0
40	0	-40	0	1.70	4.37	2.18	0.000	-90.0	2.18	0.000	-90.0
80	0	-80	0	-1.50	4.37	2.18	0.000	90.0	2.18	0.000	90.0
70	45	0	45	0.06	0.85	0.77	0.031	83.8	2.18	0.138	45.3
70	90	0	0	0.41	4.37	2.18	0.000	90.0	2.18	0.000	-89.9
80	45	0	0	-1.35	3.25	1.06	0.000	90.0	2.18	0.003	-89.9

Table B.20: Transferred Power Using Two Pairs of Dipoles With Only One Optimized

Direction of Propagation Relative to the Transmit Pair		Direction of Propagation Relative to the Receive Pair		Power Transferred		Transmit Pair Final Parameters			Receive Pair Final Parameters		
θ (deg)	ϕ (deg)	θ (deg)	ϕ (deg)	Initial (dBi)	Final (dBi)	Radiated Power (dBi)	Inverse Axial Ratio	Tilt (deg)	Radiated Power (dBi)	Inverse Axial Ratio	Tilt (deg)
0	0	0	0	4.37	4.37	2.18	0.939	-45.1	2.18	0.939	-45.0
0	0	0	0	4.37	4.37	2.18	0.998	-78.6	2.18	1.000	-1.4
45	0	-45	0	1.16	1.95	1.83	0.237	-89.5	0.58	0.618	88.6
80	0	-80	0	-1.50	1.36	2.18	0.002	90.0	-0.75	0.133	89.5
20	45	-20	0	3.60	3.61	1.83	0.804	89.2	1.80	0.911	88.4
45	45	-45	0	1.00	1.55	1.25	0.310	89.5	0.58	0.618	88.6
60	45	-60	0	-0.81	0.67	1.19	0.102	89.7	-0.16	0.408	88.8
80	45	-80	0	-2.53	0.24	1.06	0.004	90.0	-0.75	0.133	89.5